Sparse covariance fitting for source location

Luis Blanco Botana
Advisor: Montse Nájar
Universitat Politècnica de Catalunya

European Master of Research on Information and

Communication Technologies (MERIT)

4th September 2012

Abstract

This master thesis proposes a new algorithm for finding the angles of arrival of multiple uncorrelated sources impinging on a uniform linear array of sensors. The method is based on sparse signal representation and does not require either the knowledge of the number of the sources or a previous initialization. The proposed technique considers a covariance matrix model based on overcomplete basis representation and tries to fit the unknown signal powers to the sample covariance matrix. Sparsity is enforced by means of a l_1-norm penalty. The final problem is reduced to an objective function with a non-negative constraint that can be solved efficiently using the LARS/homotopy algorithm. The method described herein is able to provide high resolution with a low computational burden. It proceeds in an iterative fashion solving at each iteration a small linear system of equations until a stopping condition is fulfilled. The proposed stopping criterion is based on the residual spectrum and arises in a natural way when the LARS/homotopy is applied to the considered objective function.

Contents

Chapter 1

Introduction

1.1 Brief summary of classical direction of arrival estimators

The estimation of the Directions of Arrival (DoA) of multiple sources using sensor arrays is an old problem and plays a key role in array signal processing. During the last five decades, a plethora of methods have been proposed for finding the directions of arrival of different narrowband signals impinging on a passive array of sensors. These methods can be divided into two categories: parametric and nonparametric estimators.

Nonparametric methods include beamforming and subspace methods. The former relies on scanning the power from different locations. Exponents of this category are conventional beamformer [1] and Capon's method [2]. Conventional beamformer, a.k.a. Bartlett beamformer, suffers from poor spatial resolution and cannot resolve sources within the Rayleigh resolution limit [1]. As it is well known, this lack of resolution can be mitigated only by increasing the number of sensors of the array because improving the SNR or increasing the number of time observations does not increase the resolution. On the contrary, Capon's minimum variance method can resolve sources within the Rayleigh cell if the SNR is high enough, the number of observations is sufficient and the sources are not correlated. Unfortunately, in practice, Capon's power profile is strongly dependent on the beamwidth,

which, on its turn, depends on the explored direction and in some scenarios this could lead to a resolution loss. To counteract this, an estimator of the spectral density obtained from the Capon's power estimate was derived in [3] achieving better resolution properties. Herein this method will be referred as Normalized Capon. Another well-known category of nonparametric DoA estimators is the one composed by subspace methods. These algorithms are able to provide high-resolution and outperform beamforming methods. The most prominent member of this family is MUSIC (MUltiple SIgnals Classification) [4], it relies on an appropriate separation between signal and noise subspaces. This characterization is costly and needs a previous estimation of the number of incoming signals.

Parametric methods based on the Maximum Likelihood criterion [5] exhibit a good performance at expenses of a high computational cost. These techniques estimate the parameters of a given model instead of searching the maxima of the spatial spectrum. Unfortunately, they often lead to difficult multidimensional optimization problems with a heavy computational burden.

An interesting algorithm that lies in between the class of parametric and nonparametric techniques is the CLEAN algorithm. This method was firstly introduced by Högbom in [6] and have applications in several areas: array signal processing, image processing, radar and astronomy. Recently, Stoica and Moses throw light on the semiparametric nature of the algorithm [7]. Broadly speaking, it operates in a recursive manner substracting at each iteration a fraction of the strongest signal from the observed spatial spectrum.

For those readers interested on a more detailed and comprehensive summary of angle of arrival estimators, the authors refer them to [1] and [8].

1.2 Sparse signal representation in source location

Sparse representation of signals over redundant dictionaries is a hot topic that has attracted the interest of researchers in many fields during the last decade, such as image reconstruction [9], variable selection [10] and compressed sensing [11]. The most basic problem aims to find the sparsest vector $\mathbf{x}$ such

that $\mathbf{y} = \mathbf{A}\mathbf{x}$, where $\mathbf{y}$ is the measured vector and $\mathbf{A}$ is known. This matrix $\mathbf{A}$ is called dictionary and is overcomplete, i.e., it has more columns than rows. As a consequence, without imposing an sparsity prior on $\mathbf{x}$, the set of equations $\mathbf{y} = \mathbf{A}\mathbf{x}$ is underdetermined and admits many solutions. Formally, the objective is to minimize $\|\mathbf{x}\|_0$ subject to $\mathbf{y} = \mathbf{A}\mathbf{x}$, where $\|\cdot\|_0$ denotes the so-called l_0-norm [12], the counting function $\|\cdot\|_0 : \mathbb{R}^N \longrightarrow \mathbb{R}$ that returns the number of nonzero components in its argument. This problem is an intractable NP-hard combinatorial problem in general [13]. Fortunately, recent publications show that if the vector is sufficiently sparse the problem can be relaxed replacing the l_0-norm by a l_1-norm [13], leading to less computationally demanding convex optimization problems. The conditions that ensure the uniqueness of the solution were studied in [14]. In this context, LASSO (Least Absoulte Shrinkage and Selection Operator) [15] is a powerful tool. In its unconstrained formulation LASSO can be formally expressed as the minimization of $\|\mathbf{y} - \mathbf{A}\mathbf{x}\|_2^2 + \tau \|\mathbf{x}\|_1$, being τ a regularization parameter which balances the tradeoff between the fidelity of the representation with the measured vector and the sparsity of the solution. This problem is also known as basis pursuit denoising [16] and can be solved efficiently using the LARS/homotopy algorithm [17], [18] and [19]. Briefly, this algorithm proceeds in a iterative fashion jumping from vertex to vertex of the solution path by adding or removing entries in the solution vector.

Although there are some pioneering studies carried out in the late nineties, e.g. [20] and [21], the application of sparse representation to direction finding has gained noticeable interest during the last decade. Recent techniques based on sparse representation show promising results that outperform conventional high-resolution methods such as MUSIC. In [20] a recursive weighted minimum-norm algorithm called FOCUSS was presented. This algorithm considers a single snapshot and requires a proper initialization. The extension to the multiple-snapshot case was carried out in [22] and it is known as M-FOCUSS. Unfortunately, as it is described in [23], this technique is computationally expensive and requires the tuning of two hyperparameters that can affect the performance of the method significantly.

If multiple snapshots can be collected in an array of sensors, they can be used to improve the estimation of the angles of arrival. Several approaches for summarizing multiple observations have been proposed in the literature. The first of these approaches is the so-called l_1-SVD presented by Malioutov

et al. in [24]. This method is based on the application of a Singular Value Decomposition (SVD) over the received data matrix and leads to a second order cone optimization problem. This algorithm requires an initial estimation of the number of sources. Although it does not have to be exact, a small error is needed for a good performance. An underestimation or an overestimation of the number of sources provokes a degradation in the performance of the method. Even if the effect of an incorrect determination of the number of sources has no catastrophic consequences, such as the disappearance of the sources in MUSIC, the performance of the algorithm can be considerably degraded. Another important drawback is that l_1-SVD depends on a user-defined parameter which is not trivial to select. An alternative approach to summarize multiple snapshots is the use of mixed norms over Multiple Measurement Vectors (MMV) that share the same sparsity pattern ([22], [25]). This formulation is useful in array signal processing, specially, when the number of snapshots is smaller than the number of sensors. If we assume that the snapshots are collected during the coherence time of the angles, the position of the sources keep identical among the snapshots; the only difference between them resides in the amplitudes of the impinging rays. Basically, this approach, which is out of the scope of the paper, tries to combine multiple snapshots using the l_2 norm and to promote sparsity on the spatial dimension by means of the l_1-norm. Unfortunately, this joint optimization problem is complex and requires a high computational burden. When the number of snapshots increases, the computational load becomes too high for practical real-time source location. Recently, new techniques based on a covariance matrix fitting approach have been considered to summarize multiple snapshots, e. g. [26], [27] and [28]. Basically, these methods try to fit the covariance matrix to a certain model. The main advantage of covariance fitting approaches is that they lead to convex optimization problems with an affordable computational burden. Moreover, they do not require a previous estimation of the number of incoming sources or heavy computations such as SVD of the data. It should be also pointed out that as these methods work directly with the covariance matrix less storage space is needed because they do not need to store huge amounts of time data. The technique proposed by T. Yardibi et al. in [26] leads to an optimization problem that can be solved efficiently using Quadratic Programming (QP). In the case of the approach exposed by J. S. Picard et al. in [27], the solution is obtained by means of Linear Programming (LP). The main drawback of this last method is that it depends on a user defined parameter that is difficult to adjust. In the

same way, the authors of [29] propose a new method which is based on a hyperparameter that has been heuristically determined. On the contrary, Stoica et al. propose in [28] and [30] an iterative algorithm named SPICE (SParse Iterative Covariance-based Estimation approach), that can be used in noisy data scenarios without the need for choosing any hyperparameter. The major drawback of this method is that it needs to be initialized.

1.3 Master thesis contribution

This master thesis proposes a simple, fast and accurate algorithm for finding the angles of arrival of multiple sources impinging on a uniform linear array. In contrast to other methods in the literature, the proposed technique does not depend on user-defined parameters and does not require either the knowledge of the number of sources or initialization. It assumes white noise and that the point sources are uncorrelated.

The method considers a structured covariance matrix model based on over-complete basis representation and tries to fit the unknown signal powers of the model to the sample covariance. Sparsity is promoted by means of a l_1-norm penalty imposed on the powers. The final problem is reduced to an objective function with a non-negative constraint that can be solved efficiently using the LARS/homotopy algorithm, which is, in general, faster than QP [19] and LP [17]. The method described herein proceeds in an iterative manner solving at each iteration a small linear system of equations until a stopping condition is fulfilled. The proposed stopping criterion is based on the residual spectrum and arises in a natural way when the LARS/homotopy is applied to the considered objective function. From the best of our knowledge this stopping condition has never been considered before in sparse signal representation.

Chapter 2

Classical methods for source location

2.1 Conventional (Bartlett) beamforming

Conventional beamformer is a natural extension of the classical Fourier-based spectral analysis to sensor arrays. It relies on scanning the power coming from different locations. The directions of arrival are given by the highest peaks of the classical spatial spectrum, computed as:

$$\mathbf{P}_{BF}(\theta) = \frac{\mathbf{s}^H(\theta)\,\hat{\mathbf{R}}\mathbf{s}(\theta)}{\mathbf{s}^H(\theta)\,\mathbf{s}(\theta)} \tag{2.1}$$

where $\mathbf{s}(\theta)$ denotes the steering vector associated to the explored angle θ and $\hat{\mathbf{R}}$ is the spatial sample covariance matrix obtained from a set of N observations $\hat{\mathbf{R}} = \frac{1}{N}\sum_{k=1}^{N}\mathbf{y}[k]\,\mathbf{y}^H[k]$.

In Uniform Linear Arrays (ULA), the denominator of (2.1) becomes $\mathbf{s}^H(\theta)\,\mathbf{s}(\theta) = M$. Thus, omitting the constant term in the denominator the next expression is obtained:

$$\mathbf{P}_{BF-U}(\theta) = \mathbf{s}^H(\theta)\,\hat{\mathbf{R}}\mathbf{s}(\theta) = \frac{1}{N}\sum_{k=1}^{N}\left|\mathbf{s}^H(\theta)\,\mathbf{y}[k]\right|^2 \tag{2.2}$$

Note that conventional beamformer can be intrepeted as an average of "spatial periodograms" over the available snapshots. As it is well-known, it exhibits a poor spatial resolution and cannot resolve sources within the Rayleigh limit. Actually, the Bartlett beamforming is independent of the scenario and this lack of resolution can be increased only by increasing the number of sensors in the array because improving the SNR or increasing the number of observations does not change the resolution.

2.2 Capon's method and Normalized Capon

The Capon's method, a.k.a. Minimum Variance Distortionless Response (MVDR), is another exploration technique. Basically, this technique attempts to minimize the power contributed by noise and any other signals coming from other angles of arrival different than the explored direction. The angles of arrival are given by the locations of the largest peaks of Capon's power profile, given by:

$$\mathbf{P}_{CAP}(\theta) = \frac{1}{\mathbf{s}^H(\theta)\,\hat{\mathbf{R}}^{-1}\mathbf{s}(\theta)} \tag{2.3}$$

Capon's method outperforms the traditional Bartlett's estimator. It can resolve sources within the Rayleigh cell if the SNR is high enough, the number of snapshots is sufficient and the sources are not correlated. However, in practice, the estimation depends strongly on beamwidth, which, on its turn, depends on the explored direction and in some scenarios this could lead to a resolution loss. To counteract this undesired effect an estimator of the spectral density was proposed in [3].

$$\mathbf{P}_{NCAP}(\theta) = \frac{\mathbf{s}^H(\theta)\,\hat{\mathbf{R}}^{-1}\mathbf{s}(\theta)}{\mathbf{s}^H(\theta)\,\hat{\mathbf{R}}^{-2}\mathbf{s}(\theta)} \tag{2.4}$$

This method outperforms the Capon's method and will be referred herein as Normalized Capon (NCapon).

2.3 Subspace methods: MUSIC

The MUSIC method relies on the eigenvalue decomposition of the spatial covariance matrix. As the covariance matrix $\mathbf{R}$ is an hermitian matrix, the following properties hold: the eigenvalues are real-valued and the eigenvectors form an orthonormal set (see [7] for further information). Bearing in mind this two properties, it follows:

$$\mathbf{RU} = \mathbf{U\Lambda} \tag{2.5}$$

where $\mathbf{U}$ is a unitary matrix, that is, $\mathbf{U}^H\mathbf{U} = \mathbf{U}\mathbf{U}^H = \mathbf{I}$ and $\mathbf{\Lambda}$ is a diagonal matrix $\mathbf{\Lambda} = diag(\lambda_1, \cdots, \lambda_M)$ that contains the ordered real eigenvalues of $\mathbf{R}$ such that $\lambda_1 \geqslant \lambda_2 \geqslant \cdots \geqslant \lambda_M \geqslant 0$. Taking into account (2.5), the spatial covariance matrix admits the following decomposition:

$$\mathbf{R} = \mathbf{S}\left(\boldsymbol{\theta}\right)\mathbf{P}\mathbf{S}^H\left(\boldsymbol{\theta}\right) + \sigma_w^2\mathbf{I}_M = \mathbf{U\Lambda U}^H \tag{2.6}$$

Observe that any vector orthogonal to $\mathbf{S}\left(\boldsymbol{\theta}\right)$ is an eigenvector of $\mathbf{R}$ with eigenvalue σ_w^2. There are $M - L$ linerly independent vectors orthogonal to $\mathbf{S}\left(\boldsymbol{\theta}\right)$ and constitute the so-called noise subspace. Since the remaining eigenvalues are larger than σ_w^2, the eigenvectors can be separated into the ones associated to noise (which correspond to eigenvalues $\lambda_{L+1} = \lambda_{L+2} = \cdots = \lambda_M = \sigma_w^2$) and those associated to signal which satisfy $\lambda_1 \geqslant \lambda_2 \geqslant \cdots \geqslant \lambda_L \geqslant \sigma_w^2$. This information is used to separate $\mathbf{U}$ into noise and signal subspaces $\mathbf{U} = [\mathbf{U}_s\ \mathbf{U}_n]$. In this way, the expression (2.6) can be rewritten as:

$$\mathbf{R} = \mathbf{U\Lambda U}^H = \mathbf{U}_s\mathbf{\Lambda}_s\mathbf{U}_s^H + \mathbf{U}_n\mathbf{\Lambda}_n\mathbf{U}_n^H \tag{2.7}$$

where $\mathbf{\Lambda}_s$ and $\mathbf{\Lambda}_n = \sigma_w^2\mathbf{I}_{M-L}$ are diagonal matrices that contain the signal and the noise eigenvalues, respectively. Due to the orthogonality between subspaces, the noise subspace is orthogonal to the steering vectors corresponding to the directions of arrival of the incoming signals, that is, $\mathbf{U}_n^H\mathbf{s}(\theta) = 0$. Using this fact, the directions of arrival are given by the largest peaks of the MUSIC pseudospectrum:

$$\mathbf{P}_{MUSIC}\left(\theta\right) = \frac{1}{\mathbf{s}^H\left(\theta\right)\mathbf{U}_n\mathbf{U}_n^H\mathbf{s}\left(\theta\right)} \tag{2.8}$$

Note that in constrast with the other methods that has been discussed previously, the expression presented in (2.8) does not have a direct relation to the power; it simply exhibits sharp peaks at the directions of arrival where the sources are located.

2.3.1 Determination of the number of signals in narrowband direction finding

Many high-resolution techniques, e. g. MUSIC, rely on an adequate separation of signal and noise subspaces. This separation has a high computational burden and requires the knowledge of the number of incoming sources. Unfortunately, in practice the number of incoming signals is not known *a priori* and needs to be estimated. Furthermore, it cannot be determined directly from the multiplicity of smallest eigenvalue of $\mathbf{R}$. The main problem is that the covariance matrix is unknown and when it is estimated from a finite set of snapshots, the resulting eigenvalues are all different with probability one (actually, the smallest eigenvalues of the sample covariance is always smaller than the noise power [31]). This fact makes difficult to determine the number of impinging signals.

A plethora of techniques have been proposed in the literature for the estimation of the number of signals. The most commonly referred techniques are the so-called information theoric criteria. Exponents of this class are Akaike Information Criterion (AIC) [32] and Minimum Description Length (MDL) [33]. In these methods the number of sources is obtained maximizing the following objective function:

$$\hat{L} = \max_{L} \; J(L) \; + \rho(L) \tag{2.9}$$

where $J(L) \; = N \left[\sum_{k=L+1}^{M} \ln \lambda_k \right] - (M-L) N \ln \left[\frac{1}{M-L} \sum_{k=L+1}^{M} \lambda_k \right]$ is the loglikelihood estimate of L and the penalty function $\rho(L)$ takes the form:

$$\rho(L) = \begin{cases} 2L(2M-L) & \text{for AIC} \\ \frac{1}{2} L(2M-L) \log N & \text{for MDL} \end{cases} \tag{2.10}$$

A detailed description of information theoric criteria is out of the scope of this document, further information about model order selection techniques is provided in [34], [7].

As it is reported in [7], AIC tends to overestimate the number of sources, even at high SNR. On the contrary, the MDL criterion tends to underestimate the order at low or moderate signal to noise ratio with a finite number of snapshots. An overestimation of the number of sources in the MUSIC method is less critical than a underestimation as will be explained next. An overestimation of the size of the signal subspace will lead to a performance degradation, but if the SNR is high enough and the number of snapshots is sufficient, the algorithm will exhibit the peaks at the locations of the sources. On the contrary, if the number of sources is underestimated, the degradation in the performance of the method will be dramatic and could provoke the loss of some signal peaks. For this reason to carry out the simulations in Chapter 5 AIC will be considered to determine the number of sources in the MUSIC method.

2.4 The CLEAN algorithm

An algorithm that is closely connected to the method proposed in this thesis is the CLEAN algorithm. It was initially introduced in the mid-1970s by Högbom [6] as a deconvolution tool to mitigate sidelobe effects in radio astronomy. A significant literature can be found about CLEAN in this field (see for example [6], [35] and their references). However, the use of CLEAN is not limited to astronomy, the algorithm has been applied to diverse areas such as image processing [36], [37], [38], radar [39], spectral analysis [40], [41] and array processing [42]. From the direction-of-arrival point of view some limited research was done in [7] and [8].

It was introduced in [6] in a nonparametric fashion and assume uncorrelated point sources. The algorithm operates in a recursive manner removing at each iteration a fraction of the strongest signal from the observed spatial spectrum. The method consists of the following steps:

1. The method starts with an estimation of the Bartlett spectrum $\hat{P}_0(\theta) = \mathbf{s}^H(\theta)\,\hat{\mathbf{R}}\mathbf{s}(\theta)$, this constitutes the so-called dirty spectrum.

2. Locate the maximum of the spatial spectrum. A peak in the Bartlett spectrum indicates a direction corresponding to a source or several closely-spaced sources. Let

$$\hat{\theta}_0 = \arg\max_{\boldsymbol{\theta}} \hat{P}_0(\theta) \tag{2.11}$$

$$\hat{\sigma}_0^2 = \frac{\hat{P}_0(\theta)}{M^2} \tag{2.12}$$

   being M the number of sensors

3. Remove a fraction of the strongest signal and create the so-called residual spectrum $\hat{P}_1(\theta)$.

$$\hat{P}_1(\theta) = \hat{P}_0(\theta) - \alpha\hat{\sigma}_0^2 \left|\mathbf{s}^H(\theta)\,\mathbf{s}(\hat{\theta}_0)\right|^2 \tag{2.13}$$

   where α is the loop gain and tries to prevent the propagation of errors through the algorithm. It is a user defined parameter that fulfills $0 < \alpha < 1$ (See Section 6.5.7 of [7]). The main raison for the selection of an α lower than 1 is that if the maximum of the spatial spectrum is due to several closed-spaced sources, a cluster, to remove only an small part of the maximum of the spectrum will leave some power at and around $\hat{\theta}_0$. This will let the algorithm the possibility of resolve true sources in future iterations. There are not clear guidelines in how to choose the parameter, [7] suggests $\alpha \in [0.1, 0.25]$.

4. Iterate the procedure until an stopping criterion is fulfilled and obtain the new residual spectrum $\hat{P}_k(\theta)$ at each step, being k the index of the iteration.

The algorithm must be halted by some stopping condition. Different criteria are exposed in the literature [41]:

- To iterate a predefined number of iterations [7]. This criterion is useful in some applications where the result is insensitive to over-iteration, such as image processing.

- An stopping criterion based on some misfit to the data.
- To stop when the maximum of the residual drops below a predefined threshold. The definition of the threshold level is critical and is based on ad-hoc or heuristic criteria. Any contribution below that level is atributed to noise. In some papers this is referred as "to halt when the residual spectrum looks like noise".
- To iterate until the residual spectrum becomes too negative at some components [7].

Recently, P. Stoica and R. Moses have thrown light on the semiparametric nature of CLEAN [7] deriving the algorithm in an alternative fashion. This approach is called semiparametric because the number of incoming signals is assumed to be unkonwn and no assumptions are made regarding noise. The following spatial covariance model is considered:

$$\mathbf{R} = \sum_{i=0}^{L-1} \sigma_i^2 \mathbf{s}\left(\theta_i\right) \mathbf{s}^H\left(\theta_i\right) + \mathbf{R}_w \tag{2.14}$$

whith L unknown. The only assumption made in (2.14) is that the incoming signals are uncorrelated. Fitting the sample covariance $\hat{\mathbf{R}}$ to the model in a least square sense it results:

$$\min_{\left\{\sigma_i^2, \theta_i\right\}} \left\| \hat{\mathbf{R}} - \sum_{i=0}^{L-1} \sigma_i^2 \mathbf{s}\left(\theta_i\right) \mathbf{s}^H\left(\theta_i\right) \right\|_F^2 \tag{2.15}$$

The CLEAN algorithm is a sequential algorithm for approximately minimizing the expression (2.15). Let us start estimating the pair (σ_0^2, θ_0) by minimizing (2.15), considering $\sigma_1^2 = \sigma_2^2 = \sigma_3^2 = \cdots = 0$. Formally, this can be expressed as:

$$\min_{\sigma_0^2, \theta_0} \left\| \hat{\mathbf{R}} - \sigma_0^2 \mathbf{s}\left(\theta_0\right) \mathbf{s}^H\left(\theta_0\right) \right\|_F^2 \tag{2.16}$$

In chapter 6 of [7] it is proved that the solution of (2.16) is $\hat{\theta}_0 = \arg\max_{\boldsymbol{\theta}} \hat{P}_0(\theta)$ and $\hat{\sigma}_0^2 = \frac{\hat{P}_0(\theta)}{M^2}$, where $\hat{\mathbf{P}}_0(\theta) = \mathbf{s}^H\left(\theta\right) \hat{\mathbf{R}} \mathbf{s}\left(\theta\right)$.

Instead of substracting $\hat{\sigma}_0^2 \mathbf{s}^H(\theta_0)\,\mathbf{s}(\theta_0)$ in expression (2.16), let us remove a fraction $\alpha\hat{\sigma}_0^2 \mathbf{s}^H(\theta_0)\,\mathbf{s}(\theta_0)$ with $\alpha \in [0,1)$ to let the residual spatial covariance matrix $\hat{\mathbf{R}} - \alpha\hat{\sigma}_0^2 \mathbf{s}^H(\theta_0)\,\mathbf{s}(\theta_0)$ to be positive definite. Being α the loop gain described above. Next, estimate the pair (σ_1^2, θ_1) by minimizing (2.15), considering $\sigma_2^2 = \sigma_3^2 = \cdots = 0$.

$$\min_{\sigma_1^2,\theta_1} \left\| \hat{\mathbf{R}} - \alpha\hat{\sigma}_0^2 \mathbf{s}(\theta_0)\,\mathbf{s}^H(\theta_0) - \sigma_1^2 \mathbf{s}(\theta_1)\,\mathbf{s}^H(\theta_1) \right\|_F^2 \tag{2.17}$$

It is easy to prove that the solution is:

$$\hat{\theta}_1 = \arg\max_{\boldsymbol{\theta}} \hat{P}_1(\theta) \text{ and } \hat{\sigma}_1^2 = \frac{\hat{P}_1(\theta)}{M^2} \tag{2.18}$$

being $\hat{P}_1(\theta) = s^H(\theta)\left[\hat{\mathbf{R}} - \alpha\hat{\sigma}_0^2 \mathbf{s}(\theta_0)\,\mathbf{s}^H(\theta_0)\right] s(\theta)$. It is straightforward to rewrite this as the expression (2.13). Note that $\hat{P}_1(\theta)$ is the Bartlett estimator applied over the residual covariance matrix after the first iteration of the algorithm, that is, over $\hat{\mathbf{R}}_1 = \hat{\mathbf{R}} - \alpha\hat{\sigma}_0^2 \mathbf{s}(\theta_0)\,\mathbf{s}^H(\theta_0)$. Iterating the procedure the traditional CLEAN method is obtained.

The CLEAN method is summarized in Algorithm 1.

Algorithm 1 The CLEAN procedure

INITIALIZATION: $\hat{\mathbf{R}}_0 = \hat{\mathbf{R}}$
$k = 0$
while $\neq$stopping criterion **do**
  $\hat{P}_k(\theta) = \mathbf{s}^H(\theta)\,\hat{\mathbf{R}}_k \mathbf{s}(\theta)$
  $\hat{\theta}_k = \arg\max_\theta \hat{P}_k(\theta)$
  $\hat{\sigma}_k^2 = \frac{\hat{P}_k(\theta)}{M^2}$
  $\hat{\mathbf{R}}_{k+1} = \hat{\mathbf{R}}_k - \alpha\hat{\sigma}_k^2 \mathbf{s}(\hat{\theta}_k)\mathbf{s}^H(\hat{\theta}_k)$
  $k = k + 1$
end while

Although the original method is quite old, the theoretical understanding of algorithm is relatively poor. Appart from a preliminary study carried out by Schwarz in [43], is difficult to find a statistical analysis of the method in the literature. Therein the author investigated the conditions for the converge of CLEAN to a unique solution. Basically, the major drawback of CLEAN is

the heuristic nature of the method. It depends upon the choice of two user defined parameters: the loop gain and the number of substractions [44]. By changing them noticeably different results can be obtained. Furthermore, both parameters have influence on the computational burden of the method.

In certain applications, such as in image, in which a reconvolution step is applied to reconstruct the image, an over-iteration is not critical. However, in other applications such as direction finding an over-iteration could probably lead to the estimation of angles with nonexistent sources. On the contrary, an underestimation could provoke the loss of directions associated to impinging signals.

Chapter 3

Sparse regularization for solving ill-posed linear inverse problems

The aim of this chapter is to describe linear ill-posed inverse problems. This type of problems are frequently encountered in many areas of sciences and engineering. In chapter 4, the classical source location problem will be re-written as a linear inverse problem that is ill-posed. The solutions of this type of problems are very sensitive to noise and regularization methods must be used to stabilize the solutions by considering some additional information about the data. The structure of the chapter is the following. Quadratic regularization, which is the classical tool for solving ill-posed problems, is mentioned first. Unfortunately, it does not lead to sparse solutions. Due to this reason, sparse regularization techniques are introduced and discussed in the context of signal representation with overcomplete basis.

3.1 Linear ill-posed inverse problems

Ill-posed problems appear frequently in many areas of science and engineering. This term was introduced in the early 20-th century by Jacques Hadamard. Consider the next linear system

$$\tilde{\mathbf{y}} = \mathbf{A}\mathbf{x} \tag{3.1}$$

where $\tilde{\mathbf{y}} \in \mathbb{R}^{M\text{x}1}$ is the measured vector, $\mathbf{A} \in \mathbb{R}^{M\text{x}N}$ is a known matrix and $\mathbf{x}$ is the unknown vector that we want to estimate. It models an inverse problem; that is, a situation where the hidden information is computed from external observations. This linear system is said to be well-posed if it satisfies the following three requirements:

1. Existence. For each $\tilde{\mathbf{y}}$, it exists a vector $\mathbf{x}$ such that $\tilde{\mathbf{y}} = \mathbf{A}\mathbf{x}$.

2. Uniqueness. The solution is unique. Formally, if $\mathbf{A}\mathbf{x}_1 = \mathbf{A}\mathbf{x}_2$, then $\mathbf{x}_1 = \mathbf{x}_2$.

3. Stability. The solution is stable with respect to perturbations in the measured vector $\tilde{\mathbf{y}}$, that is, small perturbations on $\tilde{\mathbf{y}}$ do not cause an arbitrary large perturbation in the solution. In other words, the solution depends continously on the observed data vector $\tilde{\mathbf{y}}$ in some reasonable topology.

If one or more of these conditions are not fulfilled, the linear problem is said to be ill-posed. In practice this happens when the matrix $\mathbf{A}$ is theoretically or numerically rank deficient.

The model presented in (3.1) is noiseless. This is normally an oversimplification either because of a modelling error or because a nonnegligible level of noise is normally present in the measurement. The addition of a noise term to the model (3.1) provides a mechanism for dealing with both situations. A model including an additive noise can be expressed as

$$\mathbf{y} = \tilde{\mathbf{y}} + \mathbf{n} = \mathbf{A}\mathbf{x} + \mathbf{n} \tag{3.2}$$

Many problems in signal processing can be formulated as an underdetermined linear system of equations and this will be the case of the problem addressed in the next chapter. For this reason, our discussion on ill-posed problems will be focused on this specific case.

Consider a linear system of equations that has more unknowns than equations, i.e. $N > M$. In this case, the system either has no solution or infinitely

many solutions. These two situations violate the second and the third of the Hadamard's conditions exposed above and as a consequence, an underdetermined linear system is, by definition, an ill-posed problem. To avoid the possibility of having no solution, we shall hereafter consider that the matrix $\mathbf{A}$ is full-rank, implying that its columns span the entire space $\mathbb{R}^M$. If we have infinitely many possible solutions $\mathbf{x}$ of (3.1), among which there are some that may "look" better than the others. Then, how can we find the proper $\mathbf{x}$? As the matrix $\mathbf{A}$ cannot be directly inverted, an alternative objective function must be defined to solve the inverse problem. The goal is to find a functional that measures how close the predicted data fits the measurement. The standard approach is to minimize the Euclidean distance between the observed data and the predicted data from the model. Formally, this can be expressed as

$$\hat{\mathbf{x}} = \min_{\mathbf{x}} \|\mathbf{y} - \mathbf{A}\mathbf{x}\|_2^2 \tag{3.3}$$

The solution of this problem is well-known and is given by

$$\hat{\mathbf{x}} = \mathbf{A}^{\#}\mathbf{y} \tag{3.4}$$

where $\mathbf{A}^{\#}$ denotes the Moore-Penrose pseudo-inverse $\mathbf{A}^{\#} = (\mathbf{A}^T\mathbf{A})^{-1}\mathbf{A}^T$. Unfortunately in presence of noise in the measurement, if the condition number of $\mathbf{A}^{\#}$ (the ratio between the largest and the smallest singular value) is too large, the application of the pseudo-inverse could lead to a solution dominated by noise. Let us analyze hereafter more deeply this effect. First of all, consider the Singular Value Decomposition (SVD) of the matrix $\mathbf{A}$

$$\mathbf{A} = \mathbf{U}\mathbf{\Sigma}\mathbf{V}^T = \sum_{i=1}^{M} \lambda_i \mathbf{u}_i \mathbf{v}_i^T \tag{3.5}$$

being $\mathbf{U}$ and $\mathbf{V}$ square matrices of dimensions M and N, respectively, and $\mathbf{\Sigma}$ a M x N matrix. Furthermore, $\mathbf{U}$ and $\mathbf{V}$ are unitary matrices. Therefore, $\mathbf{U}\mathbf{U}^T = \mathbf{I}_M$ and $\mathbf{V}\mathbf{V}^T = \mathbf{I}_N$, where $\mathbf{I}_M$ denotes the identity matrix of size M. Bearing in mind (3.5), the pseudo-inverse is given by

$$\mathbf{A}^{\#} = \mathbf{V}\mathbf{\Sigma}^{\#}\mathbf{U}^T = \sum_{i=1}^{M} \lambda_i^{-1} \mathbf{v}_i \mathbf{u}_i^T \tag{3.6}$$

By applying the pseudoinverse we can find the minimum least squares solution. Recalling (3.2), (3.5) and (3.6), it yields:

$$\hat{\mathbf{x}} = \mathbf{A}^{\#}\mathbf{y} = \left[\sum_{j=1}^{M} \lambda_j^{-1}\mathbf{v}_j\mathbf{u}_j^T\right]\left[\sum_{i=1}^{M} \lambda_i\mathbf{u}_i\mathbf{v}_i^T\right]\mathbf{x} + \sum_{i=1}^{M} \lambda_i^{-1}\mathbf{v}_i\mathbf{u}_i^T\mathbf{n} \tag{3.7}$$

Let us analyze this expression. If the noise is white, the power distribution of the noise on all the left singular values of $\mathbf{A}$ is uniform and as consequence $E\{\left|\mathbf{u}_i^T\mathbf{n}\right|^2\}$ is not a function of i. By applying the pseudo-inverse, noise components are multiplied by the inverses of the eigenvalues. This is critical if the condition number of $\mathbf{A}^{\#}$ is large, because the amplification of the noise components will dominate the final solution and the signal component of interest will become hidden under the noise level.

To obtain a meaningful solution of an ill-posed problem we need to consider the so-called regularization methods. Much effort has been devoted in the last decades in the field of discrete ill-posed problems to find an appropiate solution less sensitive to noise. These methods incorporate some *a priori* information about the problem. A possible way of regularizing ill-posed inverse problems is to impose a constraint on the norm of the solution. If the coefficients of $\mathbf{x}$, denoted by $\mathbf{x}_j$ with $j = 1, ..., N$, remain unconstrained they are more susceptible to exhibit a high variance. By controlling the norm of the solution, we can control how large the coefficients grow. This problem can be formulated as

$$\min_{\mathbf{x}} \quad \|\mathbf{y} - \mathbf{A}\mathbf{x}\|_2^2 \quad \text{s.t.} \quad \|\mathbf{x}\|_p^p \leqslant \beta \tag{3.8}$$

where $\|\mathbf{x}\|_p = \left[\sum_i |\mathbf{x}_i|^p\right]^{1/p}$, with $p \geqslant 0$, denotes the so-called l_p-norm. Consequently, $\|\mathbf{x}\|_p^p = \sum_i |\mathbf{x}_i|^p$. Figure 3.1 shows the geometry of l_p norm for $p = 0.5, 1, 2, 3$.

The classical approach to regularize ill-posed problems is to control the energy of the solution using the squared Euclidean norm ($p = 2$):

$$\min_{\mathbf{x}} \quad \|\mathbf{y} - \mathbf{A}\mathbf{x}\|_2^2 \quad \text{s.t.} \quad \|\mathbf{x}\|_2^2 \leqslant \beta \tag{3.9}$$

This problem is the so-called Tykhonov regularization. Introducing the Lagrangian it is easy to obtain the next closed-form solution

$$\mathbf{x}_{\lambda}^{Tikhonov} = \left(\mathbf{A}^T\mathbf{A}+\lambda\mathbf{I}_N\right)^{-1}\mathbf{A}^T\mathbf{y} \tag{3.10}$$

Where λ is a Lagrange multiplier. Note that inclusion of λ makes the problem non-singular even if $\mathbf{A}^T\mathbf{A}$ is not invertible. The use of the Euclidean norm is widespread in a plethora of fields of engineering. This is mainly due to its simplicity as it has been shown in the above closed-form solution. Nevertheless, the following question arises: is $\|\mathbf{x}\|_2^2$ the best choice in (3.8)? Well, it depends. The selection of a proper regularizer depends on the property of the solution that we want to enforce and, consequently, this depends on the particular application. Traditionally, in many mathematical problems, priors of choice are different forms of smothness or energy constraints (as in the Tykhonov problem), and the corresponding regularizers are l_2-norms of $\mathbf{x}$ or its derivatives. Unfortunately, Tykhonov regularization leads to non-sparse solutions which typically have non-zero values associated to all the coefficients. While the Tykhonov is an effective mean of achieving numerical stability and increasing predictive performance, it does not address any problem related to the parsimony of the model or the interpretability of the coefficient values. Contrary, in the last years, the use of sparsity promoting norms has attracted the interest of researchers in many areas. This is the case of l_p-norms with $0 \leqslant p \leqslant 1$ in the problem (3.8) which enforce sparsity and promote few non-zero components in the solution vector. Unfortunately, the problem (3.8) is not convex for $p < 1$ and therefore, the l_1-norm ($p = 1$) is preferred. l_1 regularization has many of the beneficial properties of the l_2 regularization but yields sparse solutions that can be more easily interpreted.

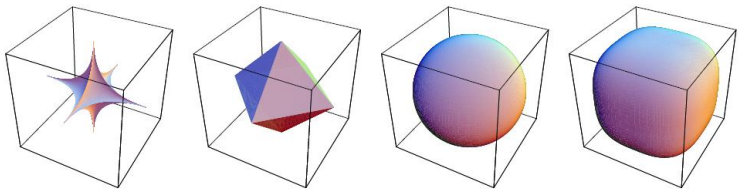

Figure 3.1: Geometry of the l_p norm in three dimensions. This figure show l_p norm for various values of p. From left to right, $p = 0.5,\ 1,\ 2,\ 3$.

3.2 Sparse signal representation

Sparse representation of signals over redundant dictionaries is a hot topic that has attracted the interest of researchers in many fields during the last decade, such as image reconstruction [9], variable selection [10] and compressed sensing [11]. The most basic problem aims to find the sparsest vector $\mathbf{x}$ such that $\mathbf{y} = \mathbf{A}\mathbf{x}$, where $\mathbf{y}$ is the measured vector and $\mathbf{A}$ is known. This matrix $\mathbf{A}$ is called dictionary and is overcomplete, i. e., it has more columns that rows. As a consequence, without imposing a sparsity prior on $\mathbf{x}$, the set of equations $\mathbf{y} = \mathbf{A}\mathbf{x}$ is underdetermined and admits many solutions. Formally, the objective is to minimize $\|\mathbf{x}\|_0$ subject to $\mathbf{y} = \mathbf{A}\mathbf{x}$, where $\|\cdot\|_0$ denotes the l_0-norm [12]. This is an intractable NP-hard combinatorial problem in general [13]. Fortunately, if the vector is sufficiently sparse the problem can be relaxed replacing the l_0-norm by a l_1-norm, defined as $\|\mathbf{x}\|_1 = \sum_i |x_i|$, leading to a convex optimization problem with a lower computational burden. The conditions that ensure the uniqueness of the solution were studied in [14].

In case of an observation vector contaminated by noise, a natural variation is to relax the equality constraint to allow some error tolerance $\varepsilon \geqslant 0$:

$$\min_{\mathbf{x}} \|\mathbf{x}\|_1 \quad \text{subject to} \quad \|\mathbf{y} - \mathbf{A}\mathbf{x}\|_2^2 \leqslant \varepsilon \tag{3.11}$$

Or alternatively,

$$\min_{\mathbf{x}} \|\mathbf{y} - \mathbf{A}\mathbf{x}\|_2^2 \quad \text{subject to} \quad \|\mathbf{x}\|_1 \leqslant \beta \tag{3.12}$$

where the constraint $\|\mathbf{x}\|_1 \leqslant \beta$ with $\beta \geqslant 0$ promotes sparsity. This formulation is known as LASSO (Least Absolute Shrinkage and Selector Operator) and was originally proposed by Tibishirani in [15]. The augmented formulation of (3.12) is well-known in signal processing and is commonly called Basis Pursuit Denoising (BPDN) [16]:

$$\min_{\mathbf{x}} \|\mathbf{y} - \mathbf{A}\mathbf{x}\|_2^2 \ + \tau \ \|\mathbf{x}\|_1 \quad \text{with} \ \ \tau \geq 0 \tag{3.13}$$

The three formulations (3.11)-(3.13) are equivalent in the sense that the sets of solutions are the same for all the possible choices of the parameters τ, ε, β. To go from one formulation to the other we only need a proper correspondence of the parameters. Nevertheless, even if the mapping between

the regularization parameters exists, this correspondence is not trivial and it is possibly non-linear and discontinous [17].

When the vector $\mathbf{x}$ is real, the LASSO problem (3.12), or its equivalent formulation (3.13), can be solved with standard quadratic programming techniques [15]. However, these techniques are time demanding and faster methods are preferred. Osborne et al. [18] and later Efron et al. [19] proposed an efficient algorithm for solving the LASSO. This algorithm is known as "homotopy method" [18] or LARS (Least Angle Regression) [19]. In this master thesis this technique will be referred to as LARS/homotopy. A variant of the traditional LASSO problem, that will be specially useful in the covariance fitting that will be addressed later on, is the so-called positive LASSO. In this case, an additional constraint over the entries of the vector $\mathbf{x}$ is considered in the LASSO problem to enforce the components of the vector to be non-negative:

$$\begin{aligned} &\min_{\mathbf{x}} \|\mathbf{y}-\mathbf{A}\mathbf{x}\|_2^2 \\ \text{subject to} \quad &\|\mathbf{x}\|_1 \leqslant \beta \quad \text{and} \quad x_i \geq 0 \ \forall i \end{aligned} \tag{3.14}$$

The positive LASSO problem (3.14) can be solved in a efficient way introducing some slight modifications in the traditional LARS/homotopy. This approach was proposed by Efron et al. in [19], but is not as widely known as the traditional one. Briefly, the algorithm starts with a very large value of τ, and gradually decreases the regularization parameter, until the desired value is attained. As τ evolves, the optimal solution for a given τ, $\mathbf{x}(\tau)$ moves on a piecewise affine path. As the minimizer $\mathbf{x}(\tau)$ is a piecewise-linear function of τ we only need to find the critical regularization parameters $\tau_0, \tau_1, \tau_2, ..., \tau_{stop}$ where the slope changes [17], these values are the so-called breakpoints. The algorithm starts with $\mathbf{x} = \mathbf{0}$ and operates in an iterative fashion calculating the critical regularization parameters $\tau_0 > \tau_1 > \cdots > \tau_{stop} \geqslant 0$ and the associated minimizers $\mathbf{x}(\tau_0)$, $\mathbf{x}(\tau_1), ..., \mathbf{x}(\tau_{stop})$ where an inactive component of $\mathbf{x}$ becomes positive or an active element becomes equal to zero. Normally, the number of active components increases as τ decreases. Nevertheless, this fact cannot be guaranteed: at some breakpoints, some entries may need to be removed from the active set.

Chapter 4

Sparse covariance fitting for source location

Consider L narrowband signals $\{x_i[k]\}_{i=1}^{L}$ impinging on an array of M sensors. The kth observation can be expressed as:

$$\mathbf{y}[k] = \mathbf{S}(\boldsymbol{\theta})\,\mathbf{x}[k] + \mathbf{w}[k] \qquad k = 1, \ldots, N \tag{4.1}$$

where $\mathbf{x}[k] = \begin{bmatrix} x_1[k] & \cdots & x_L[k] \end{bmatrix}^T$ is the vector of unknown source signals, the matrix $\mathbf{S}(\boldsymbol{\theta}) \in \mathbb{C}^{M\times L}$ is the collection of the steering vectors corresponding to the angles of arrival of the sources $\boldsymbol{\theta} = [\theta_1, \ldots, \theta_L]^T$, that is, $\mathbf{S}(\boldsymbol{\theta}) = [\mathbf{s}(\theta_1) \cdots \mathbf{s}(\theta_L)]$, and $\mathbf{w}[k] \in \mathbb{C}^{M\times 1}$ denotes a zero-mean additive noise, spatially, and temporally white, independent of the sources with covariance matrix $\sigma_w^2\mathbf{I}_M$, being $\mathbf{I}_M$ the identity matrix of size M.

Taking into account (4.1) the spatial covariance matrix can be expressed as:

$$\mathbf{R} = E\left\{\mathbf{y}[k]\,\mathbf{y}^H[k]\right\} = \mathbf{S}(\boldsymbol{\theta})\,\mathbf{P}\mathbf{S}^H(\boldsymbol{\theta}) + \sigma_w^2\mathbf{I}_M \tag{4.2}$$

being $\mathbf{P} = E\left\{\mathbf{x}[k]\,\mathbf{x}^H[k]\right\}$. The classical direction finding problem can be reformulated as a sparse representation problem. With this aim, let us consider an exploration grid of G equally spaced angles $\boldsymbol{\Phi} = \{\phi_1, \ldots, \phi_G\}$ with $G >> M$ and $G >> L$. If the set of angles of arrival of the impinging signals $\boldsymbol{\theta}$ is a subset of $\boldsymbol{\Phi}$, the received signal model (4.1) can be rewritten in terms of an overcomplete matrix $\mathbf{S}_G$ constructed by the horizontal concatenation of the steering vectors corresponding to all the potential source locations.

$$\mathbf{y}[k] = \mathbf{S}_G\mathbf{x}_G[k] + \mathbf{w}[k] \tag{4.3}$$

where $\mathbf{S}_G \in \mathbb{C}^{M\times G}$ contains the steering vectors corresponding to the angles of the grid $\mathbf{S}_G = [\mathbf{s}_1 \cdots \mathbf{s}_G]$, with $\mathbf{s}_i = \mathbf{s}(\phi_i)$, and $\mathbf{x}_G[k] \in \mathbb{C}^{G\times 1}$ is a sparse vector. The non-zero entries of $\mathbf{x}_G[k]$ are the positions that corresponds to the source locations. In other words, the nth element of $\mathbf{x}_G[k]$ is different from zero and equal to the qth component of the vector $\mathbf{x}[k]$ defined in (4.1), denoted by $x_q[k]$, if and only if $\phi_n = \theta_q$. It is important to point out that the matrix $\mathbf{S}_G$ is known and does not depend on the source locations.

The assumption that the set of angles of arrival is a subset of $\mathbf{\Phi}$ is only required for the derivation of the algorithm. Obviously, it does not always hold. Actually, this is a common assumption in many exploration methods in the direction finding literature (e.g., Capon, Normalized Capon, MUSIC, etc). In the case that $\boldsymbol{\theta} \nsubseteq \mathbf{\Phi}$, the contribution of the sources leaks into the neighboring elements of the grid.

Bearing in mind (4.3) and assuming a white noise with covariance matrix $\sigma_w^2\mathbf{I}_M$, the spatial covariance matrix of (4.1) can be rewritten in terms of $\mathbf{S}_G$ and takes the form:

$$\mathbf{R} = E\left\{\mathbf{y}[k]\,\mathbf{y}^H[k]\right\} = \mathbf{S}_G\mathbf{D}\mathbf{S}_G^H + \sigma_w^2\mathbf{I}_M \tag{4.4}$$

with $\mathbf{D} = E\left\{\mathbf{x}_G[k]\,\mathbf{x}_G^H[k]\right\}$. An important remark is that $\mathbf{D} \in \mathbb{C}^{G\times G}$ is different to the source covariance matrix $\mathbf{P} \in \mathbb{C}^{L\times L}$ introduced in (4.2). Actually, since only L^2 entries out of G^2 can differ from zero, $\mathbf{D}$ is a sparse matrix.

A common assumption in many direction finding problems is that sources are uncorrelated. Under this assumption, the matrix $\mathbf{D}$ is a diagonal matrix with only L non-zero entries given by $\mathrm{diag}(\mathbf{D}) = \begin{bmatrix} p_1 & \cdots & p_G \end{bmatrix}^T = \mathbf{p}$, being $\mathbf{p} \in \mathbb{R}_+^{G\times 1}$.

Note that $\mathbf{p}$ is a G x 1 sparse vector with non-zero entries at positions corresponding to source locations. Furthermore, the elements of $\mathbf{p}$ are real-valued and non-negative.

To cast the problem into a positive LASSO with real variables let us make some manipulations on (4.4). Applying the next property of vectorization $\mathrm{vec}\{\mathbf{ABC}\} = \mathbf{A}^T \otimes \mathbf{B}\,\mathrm{vec}\{\mathbf{B}\}$ to (4.4) it yields:

$$\mathrm{vec}\{\mathbf{R}\} = \mathbf{S}_G^* \otimes \mathbf{S}_G\,\mathrm{vec}\{\mathbf{D}\} + \sigma_w^2\ \mathrm{vec}\{\mathbf{I}_M\} \tag{4.5}$$

where $\otimes$ and $\mathrm{vec}\{\cdot\}$ denote the Kronecker product and the vectorization operator. It should be remarked that the result of $\mathbf{S}_G^* \otimes \mathbf{S}_G \in \mathbb{C}^{M^2\times G^2}$.

Since $\mathbf{D}$ is a diagonal matrix because the sources are uncorrelated, only G columns of $\mathbf{S}_G^* \otimes \mathbf{S}_G$ have to be taken into account. Using this fact, the

dimensionality of the problem can be reduced. In this way, it is straightforward to rewrite the expression (4.5) in terms of vector $\mathbf{p}$ just removing some columns of $\mathbf{S}_G^* \otimes \mathbf{S}_G$:

$$\text{vec}\{\mathbf{R}\} = \tilde{\mathbf{A}}\mathbf{p} + \sigma_w^2 \ \text{vec}\{\mathbf{I}_M\} \tag{4.6}$$

with $\tilde{\mathbf{A}} = [\ \mathbf{s}_1^* \otimes \mathbf{s}_1 \quad \mathbf{s}_2^* \otimes \mathbf{s}_2 \quad \cdots \quad \mathbf{s}_G^* \otimes \mathbf{s}_G\ ]$. Note that $\tilde{\mathbf{A}} \in \mathbb{C}^{M^2 \times G}$.

Separating real and imaginary parts the above equation takes the form:

$$\begin{bmatrix} \mathbf{r}_r \\ \mathbf{r}_i \end{bmatrix} = \begin{bmatrix} \tilde{\mathbf{A}}_r \\ \tilde{\mathbf{A}}_i \end{bmatrix} \mathbf{p} + \begin{bmatrix} \sigma_w^2 \ \text{vec}\{\mathbf{I}_M\} \\ \mathbf{0}_{M^2 \text{ x } 1} \end{bmatrix} \tag{4.7}$$

where

$$\begin{aligned} \mathbf{r}_r &= \text{Re}\{\text{vec}[\mathbf{R}]\} \quad \tilde{\mathbf{A}}_r = \text{Re}\left\{\tilde{\mathbf{A}}\right\} \\ \mathbf{r}_i &= \text{Im}\{\text{vec}[\mathbf{R}]\} \quad \tilde{\mathbf{A}}_i = \text{Im}\left\{\tilde{\mathbf{A}}\right\} \end{aligned}$$

In the expression (4.7), vec$\{\mathbf{I}_M\}$ denotes the vectorization of the identity matrix of dimensions M x M and $\mathbf{0}_{M^2 \text{ x}1}$ is a vector of zeros of size M^2 x 1.

More compactly, the expression (4.7) can be rewritten as:

$$\mathbf{r} = \mathbf{A}\mathbf{p} + \mathbf{n} \tag{4.8}$$

with obvious definitions for $\mathbf{r}$, $\mathbf{A}$, $\mathbf{p}$, and $\mathbf{n}$. Note that $\mathbf{r}$ and $\mathbf{n} \in \mathbb{R}^{2M^2 \times 1}$ and $\mathbf{A} \in \mathbb{R}^{2M^2 \times G}$.

Unfortunately, the spatial covariance matrix is unknown in practice and is normally replaced by the sample covariance matrix obtained from a set of N observations $\hat{\mathbf{R}} = \frac{1}{N} \sum_{k=1}^{N} \mathbf{y}[k]\,\mathbf{y}^H[k]$. A possible method for finding $\mathbf{p}$ is the following constrained least squares problem:

$$\begin{aligned} &\min_{\mathbf{p}} \|\hat{\mathbf{r}} - \mathbf{A}\mathbf{p}\|_2^2 \\ &\text{subject to} \quad p_i \geq 0 \quad i = 1, \ldots, G \\ &\|\mathbf{p}\|_1 = \sum_{j=1}^{G} p_j \leqslant \beta \quad \text{with} \quad \beta \geqslant 0 \end{aligned} \tag{4.9}$$

where $\hat{\mathbf{r}} = \begin{bmatrix} \text{Re}\left\{\text{vec}\left[\hat{\mathbf{R}}\right]\right\} \\ \text{Im}\left\{\text{vec}\left[\hat{\mathbf{R}}\right]\right\} \end{bmatrix}$.

Note that (4.9) is positive LASSO problem. The main idea behind (4.9) is to fit the unknown powers to the model such that the solution is sparse. The method tries to minimize the residual, or in other words, tries to maintain the fidelity of the sparse representation with the received data subject to a non-negative constraint on the powers and $\sum_{j=1}^{G} p_j \leqslant \beta$. This last constraint promotes sparsity, as it was exposed in (3.12), but also imposes a bound in the received signal power. Unfortunately, the parameter β is unknown and has to be estimated. Even worse, the solution of (4.9) is very sensitive to the parameter β, a little error in the estimation of the parameter can lead to a wrong solution vector.

Instead of solving (4.9) let us consider the next equivalent formulation:

$$\begin{aligned} &\min_{\mathbf{p}} \|\hat{\mathbf{r}} - \mathbf{A}\mathbf{p}\|_2^2 + \tau \|\mathbf{p}\|_1 \\ &\text{subject to } \ \tau \geq 0, \quad p_i \geq 0 \quad i = 1, \ldots, G \end{aligned} \tag{4.10}$$

The problems (4.9) and (4.10) are equivalent in the sense that the path of solutions of (4.9) parametrized by a positive β matches with the solution path (4.10) as τ varies. To go from one formulation to the other one we need a proper correspondence between the parameters.

The problem (4.10) can be solved with the LARS/homotopy algorithm for positive LASSO. The method operates in an iterative fashion computing the critical regularization parameters $\tau_0 > \tau_1 > \cdots > \tau_{\text{stop}} \geqslant 0$ and the associated minimizers $\mathbf{p}(\tau_0)$, $\mathbf{p}(\tau_1), \ldots, \mathbf{p}(\tau_{\text{stop}})$, where an inactive component of $\mathbf{p}$ becomes positive or an active element becomes equal to zero. Let us remark that there is only one new candidate to enter or leave the active set at each iteration (this is the "one at a time condition" described by Efron et al. [19]).

The algorithm is based on the computation of the so-called vector of residual correlations, or just residual correlation, $\mathbf{b}(\tau) = \mathbf{A}^T(\hat{\mathbf{r}} - \mathbf{A}\mathbf{p}(\tau))$ at each iteration. The method starts with $\mathbf{p} = \mathbf{0}$ which is the solution of (4.10) for all the $\tau \geqslant \tau_0 = 2 \max_i \left(\mathbf{A}^T\hat{\mathbf{r}}\right)_i$, being $\left(\mathbf{A}^T\hat{\mathbf{r}}\right)_i$ the ith component of the vector $\mathbf{A}^T\hat{\mathbf{r}}$, and proceeds in an iterative manner solving reduced-order linear systems. The whole algorithm is summarized in Algorithm 2 (see Appendix D and [19, 45] for further details). This iterative procedure must be halted when a stopping condition is satisfied. This stopping criterion, will be described in the next Section.

It should be pointed out that the least squares error of the covariance fitting method exposed in (4.10) decreases at each iteration of the LARS/homotopy algorithm. This result is justified by the next two theorems.

Theorem 1. *The sum of the powers increases monotonically at each iteration of the algorithm. Given two vectors with non-negative elements* $\mathbf{p}(\tau_{n+1})$ *and* $\mathbf{p}(\tau_n)$ *that are minimizers of (4.10) for two breakpoints* τ_{n+1} *and* τ_n *respectively, with* $\tau_n > \tau_{n+1}$*, it can be stated that* $\left\|\mathbf{p}(\tau_{n+1})\right\|_1 \geqslant \left\|\mathbf{p}(\tau_n)\right\|_1$.

Proof. See Appendix A. □

Theorem 2. *The least squares error* $\|\hat{\mathbf{r}} - \mathbf{A}\mathbf{p}(\tau)\|_2^2$ *decreases at each iteration of LARS/homotopy algorithm. Given two vectors with non-negative elements* $\mathbf{p}(\tau_n)$ *and* $\mathbf{p}(\tau_{n+1})$ *that are minimizers of (4.10) for two consecutive breakpoints* τ_n *and* τ_{n+1} *of the LARS/homotopy, with* $\tau_n > \tau_{n+1}$*, it can be stated that* $\|\hat{\mathbf{r}} - \mathbf{A}\mathbf{p}(\tau_{n+1})\|_2^2 \leqslant \|\hat{\mathbf{r}} - \mathbf{A}\mathbf{p}(\tau_n)\|_2^2$.

Proof. See Appendix B. □

4.1 Stopping criterion: the cumulative spectrum

The definition of an appropriate stopping criterion is of paramount importance because it determines the final regularization parameter τ_{stop} and consequently the number of active positions in the solution vector. In general, larger values of τ produce sparser solutions. Nevertheless, this fact cannot be guaranteed: at some breakpoints, some entries may need to be removed from the active set.

Most of the traditional approaches exposed in the literature for choosing the regularization parameter in discrete ill-posed problems are based on the norm of the residual error in one way or another, e. g. discrepancy principle, cross validation and the L-curve. Nevertheless, recent publications [46], [47] suggest the use of a new parameter-choice method based on the residual spectrum. This technique is based on the evaluation of the shape of the

Algorithm 2 Proposed method

INITIALIZATION: $\mathbf{p} = \mathbf{0}$, $\tau_0 = 2 \max_i \left(\mathbf{A}^T \hat{\mathbf{r}}\right)_i$, $n = 0$

$J = active\ set = \varnothing$, $I = inactive\ set = J^c$

while $\neq$stopping criterion and $\exists\ i \in I$ such that $b_i > 0$ **do**

1) Compute the residual correlation $\mathbf{b} = \mathbf{A}^T (\hat{\mathbf{r}} - \mathbf{A}\mathbf{p})$

2) Determine the maximal components of $\mathbf{b}$. These will be the non-zero elements of $\mathbf{p}(\tau_n)$ (active components).

$$J = \arg\max \{b_j\}, \quad I = J^c$$

3) Calculate the update direction $\mathbf{u}$ such that all the active components lead to an uniform decrease of the residual correlation (equiangular direction).

$$\mathbf{u}_J = \left(\mathbf{A}_J^T \mathbf{A}_J\right)^{-1} \mathbf{1_J}$$

4) Compute the step size γ such that a new element of the $\mathbf{b}$ becomes equal to the maximal ones ($\exists\ i \in I$ such that $b_i(\tau_{n+1}) = b_{j \in J}(\tau_{n+1})$) or one non-zero component of $\mathbf{p}$ becomes zero ($\exists\ j \in J$ such that $\mathbf{p}_j(\tau_{n+1}) = 0$).

5) Actualize $\mathbf{p} \rightarrow \mathbf{p} + \gamma \mathbf{u}$, $\tau_{n+1} = \tau_n - 2\gamma$, $n = n + 1$

end while

Fourier transform of the residual error. From the best of our knowledge, this approach has never been used as a stopping criterion in sparse representation problems. The method exposed herein is inspired in the same idea with some slight modifications. The main difference resides in the fact that no Fourier transform needs to be computed over the residual, as it will be exposed later on, the spatial spectrum of the residual arises in a natural way when the LARS/homotopy is applied to (4.10). The following result is the key point of the stopping criterion proposed in this master thesis.

Theorem 3. *When the LARS/homotopy is applied to the problem (4.10), the residual correlation obtained at the k-th iteration of the algorithm, expressed as* $\mathbf{b}(\tau_k) = \mathbf{A}^T(\hat{\mathbf{r}} - \mathbf{A}\mathbf{p}(\tau_k))$*, is equivalent to the Bartlett estimator applied to the residual covariance matrix* $\hat{\mathbf{C}}_k = \hat{\mathbf{R}} - \sum_{i=1}^{G} p_i(\tau_k)\, \mathbf{s}_i \mathbf{s}_i^H$*. Then, the i-th component of the vector of residual correlations satisfies* $\mathbf{b}_i(\tau_k) = \mathbf{s}_i^H \hat{\mathbf{C}}_k \mathbf{s}_i$.

Proof. See Appendix C □

This theorem provides an alternative interpretation of the residual correlation at the k-th iteration $\mathbf{b}(\tau_k)$ which can be seen as a residual spatial spectrum. Bearing in mind this idea and under the assumption that the noise is zero-mean and spatially white the following parameter-choice method is proposed: to stop as soon as the residual correlation resembles white noise.

Under the assumption that the noise is spatially white, the power is distributed uniformly over all the angles of arrival and the spatial spectrum has to be flat. To determine whether the residual correlation corresponds to a white noise spectrum a statistical tool has to be considered. Several tests are available in the literature to test the hypothesis of white noise. Herein the metric that will be considered to see if the residual looks like noise is:

$$c_k(l) = \frac{\sum_{i=1}^{l} |b_i(\tau_k)|}{\sum_{i=1}^{G} |b_i(\tau_k)|} \qquad l = 1, \cdots, G \tag{4.11}$$

where the subindex k denotes the k-th iteration of the LARS/homotopy algorithm, with $k = 0, \cdots, k_{stop}$. The metric c_k is a slight modification of the conventional normalized cumulative periodogram proposed by Bartlett in [48] and later by Durbin in [49] . Traditionally, the cumulative periodogram has been defined for real-valued time series. In the real case, the spectrum is symmetric and only half of the spectrum needs to be computed. However, it can be easily extended to embrace complex-valued vectors as it is shown in (4.11). Throughout this entire document c_k will be referred to as Normalized Cumulative Spectrum (NCS).

For an ideal white noise the plot of the NCS is a straight line and resembles the cumulative distribution of a uniform distribution. Thus, any distributional test, such as the Kolmogorov-Smirnov (K-S) test, can be considered to determine the "goodness of fit" between the cumulative spectrum and the theoretical straight line. In [48] Bartlett proposed the use of the Kolmogorov-Smirnov test which is based on the largest deviation in absolute value between the cumulative spectrum and the theoretical straight line. The K-S test rejects the hypothesis of white noise whenever the maximum deviation between the cumulative spectrum and the straight line is too large. On the contrary, the cumulative spectrum is considered white noise if it lies within the Kolmogorov-Smirnov limits. The upper and the lower K-S limits, as a function of index l, are given by

$$\frac{l}{G} \pm \frac{\delta}{\sqrt{MN}} \tag{4.12}$$

where $\delta = 1.36$ for the 95% confidence band and $\delta = 1.63$ for the 99% band.

Notice that the NCS does not require an accurate estimation of the noise power at the receiver. Since the cumulative spectrum (4.11) is normalized with respect to the average power at each k-th iteration, the decision metric only depends on the shape of the spatial spectrum.

The proposed stopping condition is: to stop as soon as the residual correlation resembles white noise, that is, when the NCS lies within the Kolmogorov-Smirnov limits.

Chapter 5

Numerical results

The aim of this Section is to analyze the performance of the covariance fitting method proposed in this master tesis. To carry out this objective, some simulations have been done in Matlab. Throughout the simulations, a uniform grid with 1^o of resolution has been considered for all the analyzed techniques. Furthermore, a zero-mean white Gaussian noise with power $\sigma_w^2 = 1$ has been considered. The generated source signals are uncorrelated and distributed as circularly symmetric i.i.d complex Gaussian variables with zero mean. Since the same power P will be considered for all the sources, throughout this entire section the signal to noise ratio (SNR) is defined by $SNR(dB) = 10\log_{10}(\frac{P}{\sigma_w^2})$.

To illustrate the algorithm and the new stopping condition based on the cumulative spectrum, we have considered four uncorrelated sources located at -36^o, -30^o, 30^o, 50^o that impinge on a uniform linear array (ULA) with $M = 10$ sensors separated by half the wavelength. The SNR is set to 0 dB and the sample covariance matrix is computed with $N = 600$ snapshots. Figure 5.1 and Figure 5.2 show the evolution of the normalized cumulative spectrum and the vector of residual correlations, respectively. As it is shown in Figure 1, the algorithm is stopped after 16 iterations when the NCS lies within the Kolmogorov Smirnov limits of the 99% confidence band. The final solution $\mathbf{p}$ is shown in the Figure 5.3. Note that the residual spectrum of the final solution in Figure 5.2 is almost flat and the residual correlation resembles white noise.

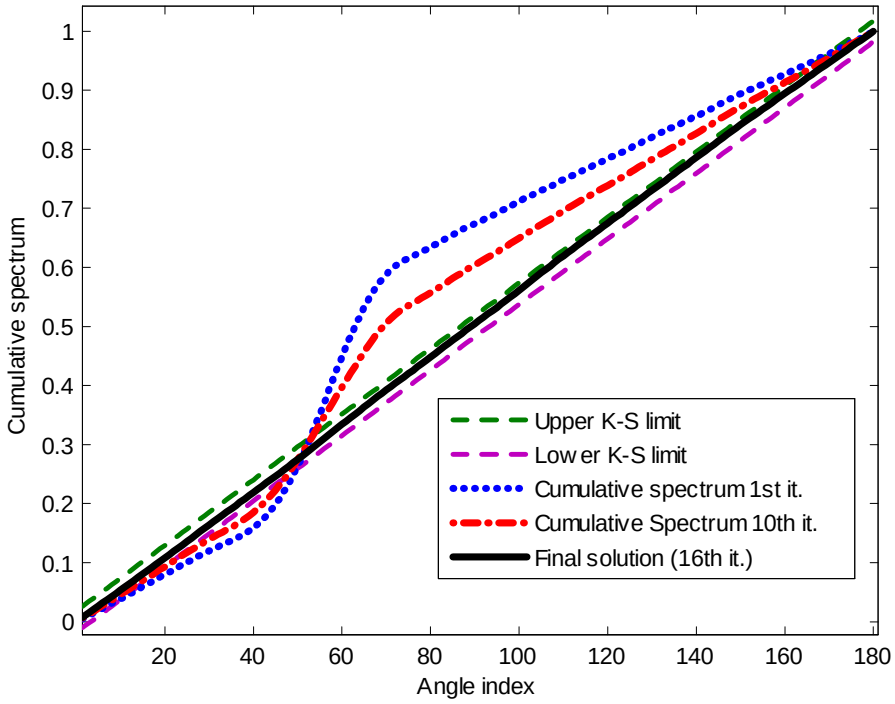

Figure 5.1: Cumulative Spectrum as a function of the angle index. The scenario is composed by four sources located at $\boldsymbol{\theta} = [-36^o, -30^o, 30^o, 50^o]$, $M = 10$ sensors, $N = 600$ snapshots, SNR $= 0$ dB. The final solution is achieved after 16 iterations of the LARS/homotopy and it is chosen as the first one that lies within the Kolmogorov-Smirnov limits of the 99% confidence band.

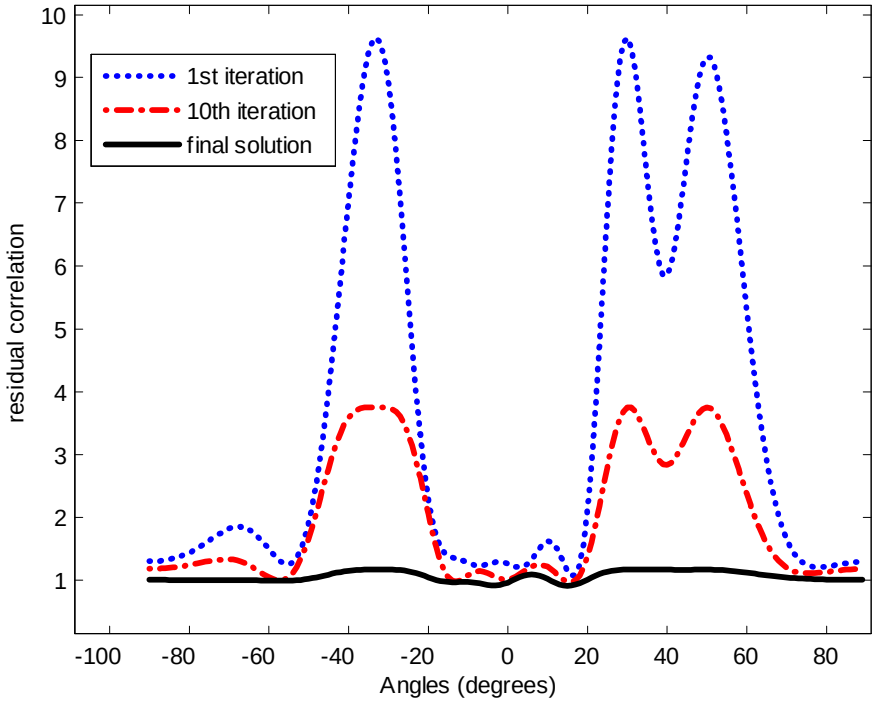

Figure 5.2: Evolution of the vector of residual correlations $\mathbf{b}$ with the iterations of the LARS/homotopy. The scenario is composed by four sources located at $\boldsymbol{\theta} = [-36^o, -30^o, 30^o, 50^o]$, $M = 10$ sensors, $N = 600$ snapshots, SNR $= 0$ dB. The final solution is achieved after 16 iterations of the LARS/homotopy and it is chosen as the first one that lies within the Kolmogorov-Smirnov limits of the 99%. Note that the residual correlation is almost flat.

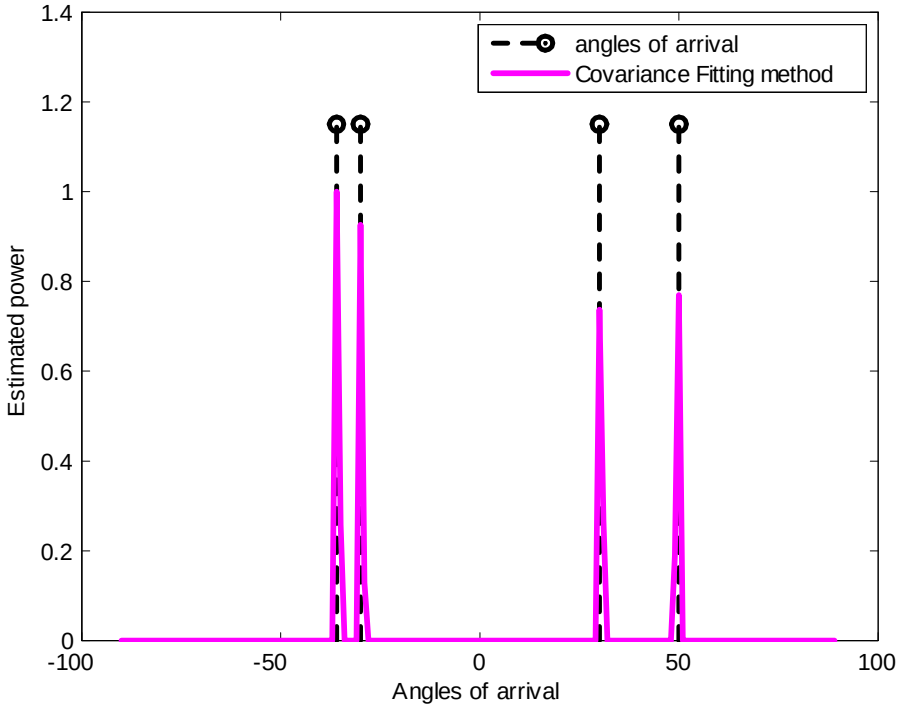

Figure 5.3: The power estimate of the proposed covariance matrix fitting method. Final solution $\mathbf{p}$ obtained by the LARS/homotopy after 16 iterations. The settings are: four sources located at $\boldsymbol{\theta} = [-36^o, -30^o, 30^o, 50^o]$, $M = 10$ sensors, $N = 600$ snapshots, SNR $= 0$ dB.

Next, the probability of resolution of the covariance fitting method as a function of the SNR is investigated. With this aim we have considered two uncorrelated sources located at -36^o and -30^o that impinge on a ULA with $M = 9$ sensors. Both sources transmit with the same power and the sample covariance has been computed with $N = 1000$ snapshots. Figure 5.4 shows the results of the covariance fitting method compared to other classical estimators: MUSIC [4], Capon [2] and Normalized Capon [3]. In order to make a fair comparison between the different techniques, the number of sources of the MUSIC algorithm has been estimated with the Akaike Information Criterion (AIC) [7]. The curves in Figure 5.4 are averaged over 300 independent simulation runs. From this figure, it is clear that the proposed covariance fitting technique outperforms the other classical estimators and it is about 6 dB better than the MUSIC algorithm and about 12 dB better than the Normalized Capon method.

Next, the perfomance of the proposed method in terms of Root Mean Square Error (RMSE) is analyzed and presented in Figure 5.5. Two uncorrelated sources separated by $\Delta\theta = 6^o$ that impinge on an array of $M = 9$ sensors were taken into account in the simulations. In this case, the positions of the sources do not correspond to the angles of the grid. With this aim, the angle of the first source θ_1 is generated as a random variable following a uniform distribution between -80^o and 80^o and the angle of the second source is generated as $\theta_2 = \theta_1 + \Delta\theta$. The sample covariance has been computed with 900 snapshots. Figure 5.5 shows the RMSE of the proposed method and MUSIC as a function of the SNR as long as the two sources are resolved with a probability equal to 1. In the case of MUSIC the determination of the number of signal sources is performed by the AIC. The two curves are based on the average of 300 independent runs. From Figure 5.5 it can be concluded that at low SNR the proposed method outperforms MUSIC. When the SNR increases both methods tends to exhibit the same performance.

Finally, the resolution capability of the method as a function of the number of snapshots is investigated. The scenario considered for this purpose is the following: two sources located at $\theta_1 = -36^o$ and $\theta_1 = -30^o$ that impinge on a ULA with $M = 9$ sensors. In this case, the transmitted signals have constant modulus, which is a common situation in communications applications, $s_1(t) = e^{j\varphi_1(t)}$ and $s_2(t) = e^{j\varphi_2(t)}$. The signal phases $\{\varphi_k(t)\}_{k=1}^2$ are independent and follow a uniform distribution in $[0, 2\pi]$. Figure 5.6 shows the probability of resolution of the proposed method and MUSIC as a function of the number of snapshots N. In this case the signal to noise ratio is fixed to

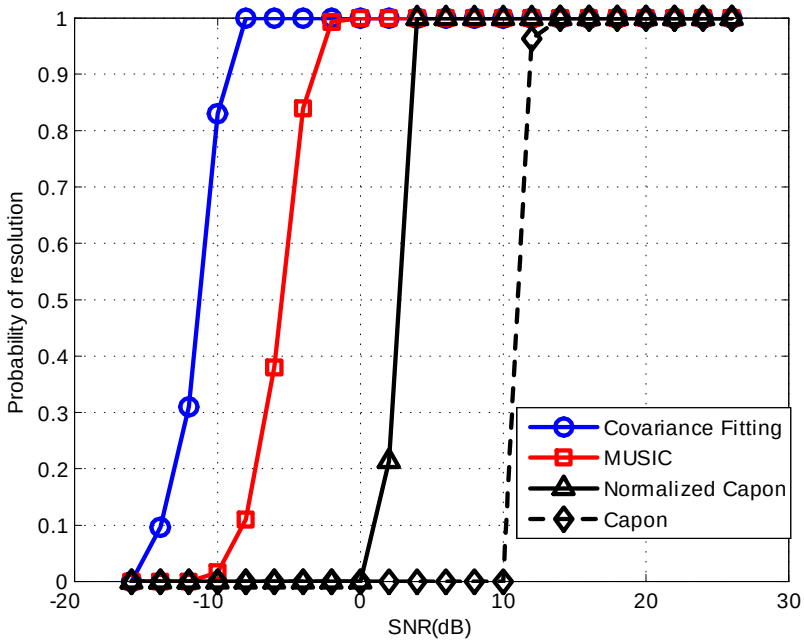

Figure 5.4: Probability of resolution against SNR. $\boldsymbol{\theta} = [-36^o, -30^o]$, $M = 9$ sensors, $N = 1000$ snapshots. The curves were obtained by averaging the results of 300 independent simulation runs.

1 dB. As in the previous cases, in order to make a fair comparison between the two techniques, the number of sources of the MUSIC algorithm has been determined using AIC. The curves were obtained by averaging the results of 500 independent trials. Note that the covariance fitting method clearly outperforms MUSIC and is able to resolve the two sources with a probability greater than 95% if $N \geqslant 30$.

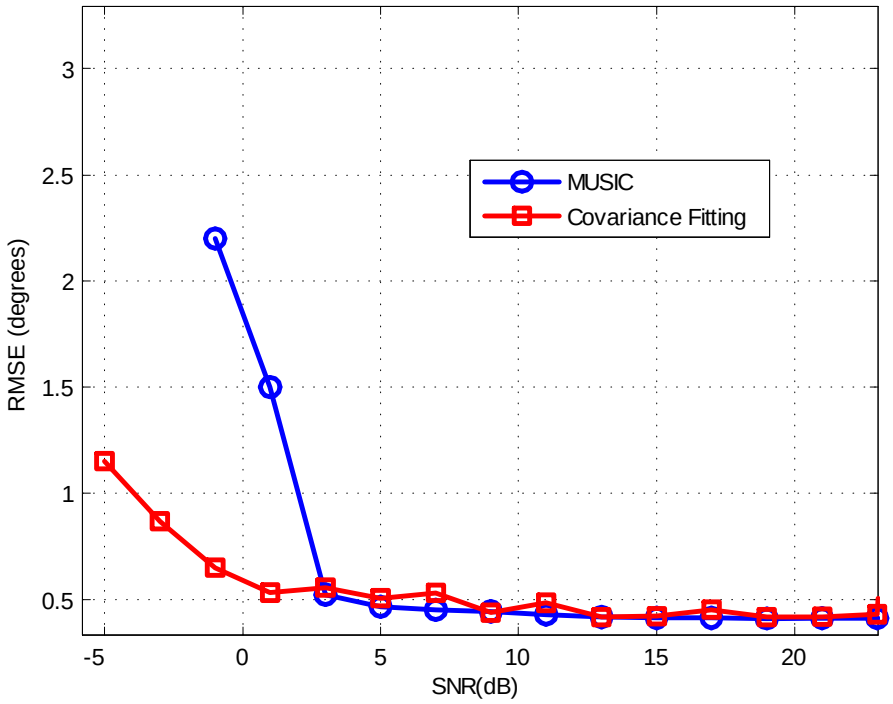

Figure 5.5: Root mean square error as a function of the signal-to-noise ratio. Two uncorrelated sources separated by $\Delta\theta = 6^o$. $M = 10$ sensors, $N = 900$ snapshots, SNR = 0 dB. The curves were obtained by averaging the results of 300 independent simulation runs.

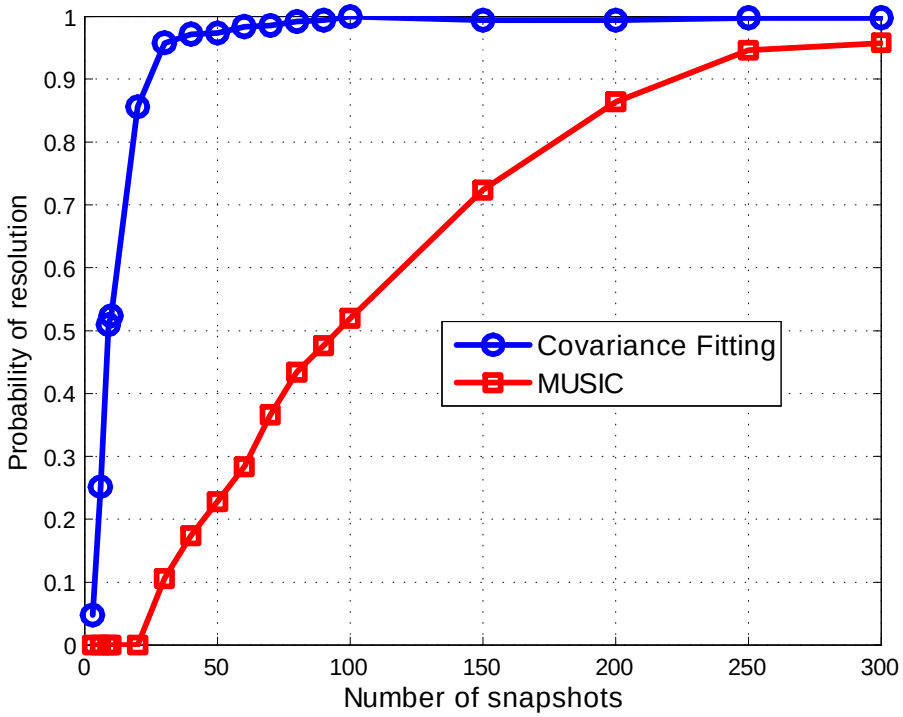

Figure 5.6: Probability of resolution as a function of the number of snapshots. Two uncorrelated sources located at $\boldsymbol{\theta} = [-36^o, -30^o]$, $M = 9$ sensors. The curves were obtained by averaging the results of 500 independent trials.

Chapter 6

Conclusions and future research lines

A new method for finding the directions of arrival of multiple sources that impinge on a ULA has been presented in this master thesis. The proposed technique is based on sparse signal representation and outperforms classical direction finding algorithms, even subspace methods, in terms of RMSE and probability of resolution. The proposed technique assumes white noise and uncorrelated point sources. Furthermore, it does not require either the knowledge of the number of sources or a previous initialization.

Related to this work, the next future lines of research are considered:

1. The **extension** of the algorithm to **correlated sources and non-linear arrays** using new algorithms for solving the linearly constrained l_1-penalized least-squares problems based on the LARS method.

2. **Frequency estimation in irregularly sampled time series.** Recently, the location of pure frequencies in the spectrum of irregularly sampled time series has attracted the interest of the researchers in several areas in the last years, such as in astrophysical data analysis. In this field, large time series of observations exhibit sampling irregularities and large observational gaps caused by the earth's rotation and the weather conditions. So far, from the best of our knowledge, the algorithms proposed for the estimation of the frequencies are based

on ad-hoc criteria based on the discretised Fourier spectrum of the residual. The use of the LARS/homotopy method jointly with the normalized cumulative periodogram provides an interesting criterion that can be investigated as a tool for the estimation of the frequencies of pure sinusoids in irregularly sampled time series.

Appendix A

Proof of theorem 1

The LARS/homotopy provides all the breakpoints $\tau_0 > \tau_1 > \cdots > \tau_{\text{stop}} \geqslant 0$ and the associated solutions $p(\tau_0), p(\tau_1), \ldots, p(\tau_{\text{stop}})$ where a new component enter or leaves the support (the set of active elements) of $p(\tau)$. It can be proved that the sum of powers increases monotonically at each iteration of the algorithm. Suppose two non-negative vectors $p(\tau_n)$ and $p(\tau_{n+1})$ that are minimizers of (4.10) for the regularization parameters τ_n and τ_{n+1}, respectively, with $\tau_n > \tau_{n+1} \geqslant 0$. The following inequality holds for the breakpoint τ_n:

$$\|\hat{\mathbf{r}} - \mathbf{A}\mathbf{p}(\tau_n)\|_2^2 + \tau_n \|\mathbf{p}(\tau_n)\|_1 \leqslant \|\hat{\mathbf{r}} - \mathbf{A}\mathbf{p}(\tau_{n+1})\|_2^2 + \tau_n \|\mathbf{p}(\tau_{n+1})\|_1 \quad (6.1)$$

Note that the regularization parameter τ_n is the same on both sides of the inequality. The expression on the right-hand side of the inequality (6.1) is equal to $\|\hat{\mathbf{r}} - \mathbf{A}\mathbf{p}(\tau_{n+1})\|_2^2 + \tau_{n+1} \|\mathbf{p}(\tau_{n+1})\|_1 + (\tau_n - \tau_{n+1}) \|\mathbf{p}(\tau_{n+1})\|_1$. Therefore, the expression (6.1) can be rewritten as:

$$\begin{aligned} \|\hat{\mathbf{r}} - \mathbf{A}\mathbf{p}(\tau_n)\|_2^2 + \tau_n \|\mathbf{p}(\tau_n)\|_1 \leqslant \|\hat{\mathbf{r}} - \mathbf{A}\mathbf{p}(\tau_{n+1})\|_2^2 + \tau_{n+1} \|\mathbf{p}(\tau_{n+1})\|_1 \\ + (\tau_n - \tau_{n+1}) \|\mathbf{p}(\tau_{n+1})\|_1 \end{aligned} \quad (6.2)$$

By using minimization properties, if $p(\tau_{n+1})$ is the minimizer of (4.10) for the regularization parameter τ_{n+1}. Then, next inequality holds:

$$\|\hat{\mathbf{r}} - \mathbf{A}\mathbf{p}(\tau_{n+1})\|_2^2 + \tau_{n+1} \|\mathbf{p}(\tau_{n+1})\|_1 \leqslant \|\hat{\mathbf{r}} - \mathbf{A}\mathbf{p}(\tau_n)\|_2^2 + \tau_{n+1} \|\mathbf{p}(\tau_n)\|_1 \quad (6.3)$$

Note that the regularization parameter τ_{n+1} is the same on both sides of the inequality. Bearing in mind (6.3) and (6.2), it is straightforward to obtain

$$\begin{aligned}\|\hat{\mathbf{r}} - \mathbf{A}\mathbf{p}(\tau_n)\|_2^2 + \tau_n \|\mathbf{p}(\tau_n)\|_1 \leqslant \|\hat{\mathbf{r}} - \mathbf{A}\mathbf{p}(\tau_n)\|_2^2 + \tau_{n+1} \|\mathbf{p}(\tau_n)\|_1 \\ +(\tau_n - \tau_{n+1}) \|\mathbf{p}(\tau_{n+1})\|_1\end{aligned} \tag{6.4}$$

If the term $\tau_n \|\mathbf{p}(\tau_n)\|_1$ is added and subtracted from expression on the right-hand side of the inequality (6.4), the next expression is obtained:

$$\begin{aligned}\|\hat{\mathbf{r}} - \mathbf{A}\mathbf{p}(\tau_n)\|_2^2 + \tau_n \|\mathbf{p}(\tau_n)\|_1 \quad \leqslant \quad \|\hat{\mathbf{r}} - \mathbf{A}\mathbf{p}(\tau_n)\|_2^2 + \tau_n \|\mathbf{p}(\tau_n)\|_1 \\ +(\tau_n - \tau_{n+1}) (\|\mathbf{p}(\tau_{n+1})\|_1 - \|\mathbf{p}(\tau_n)\|_1)\end{aligned} \tag{6.5}$$

Therefore we can conclude that $(\tau_n - \tau_{n+1})(\|\mathbf{p}(\tau_{n+1})\|_1 - \|\mathbf{p}(\tau_n)\|_1) \geqslant 0$. As $\tau_n > \tau_{n+1} \geqslant 0$, then $\|\mathbf{p}(\tau_{n+1})\|_1 - \|\mathbf{p}(\tau_n)\|_1 \geqslant 0$. Finally, we obtain $\|\mathbf{p}(\tau_{n+1})\|_1 \geqslant \|\mathbf{p}(\tau_n)\|_1$.

Appendix B

Proof of theorem 2

If $\mathbf{p}(\tau_{n+1})$ is a vector with non-negative components that minimizes the problem (4.10) for $\tau_{n+1} > 0$, then the following inequality is fulfilled:

$$\|\hat{\mathbf{r}} - \mathbf{A}\mathbf{p}(\tau_{n+1})\|_2^2 + \tau_{n+1} \|\mathbf{p}(\tau_{n+1})\|_1 \leqslant \|\hat{\mathbf{r}} - \mathbf{A}\mathbf{p}(\tau_n)\|_2^2 + \tau_{n+1} \|\mathbf{p}(\tau_n)\|_1 \quad (6.6)$$

which can be rewritten as:

$$\tau_{n+1}(\|\mathbf{p}(\tau_{n+1})\|_1 - \|\mathbf{p}(\tau_n)\|_1) \leqslant \|\hat{\mathbf{r}} - \mathbf{A}\mathbf{p}(\tau_n)\|_2^2 - \|\hat{\mathbf{r}} - \mathbf{A}\mathbf{p}(\tau_{n+1})\|_2^2 \quad (6.7)$$

Since $\tau_{n+1} > 0$ and $\|\mathbf{p}(\tau_{n+1})\|_1 - \|\mathbf{p}(\tau_n)\|_1 \geqslant 0$, as it was proved in Theorem 1, the following inequality is fulfilled $\|\hat{\mathbf{r}} - \mathbf{A}\mathbf{p}(\tau_n)\|_2^2 - \|\hat{\mathbf{r}} - \mathbf{A}\mathbf{p}(\tau_{n+1})\|_2^2 \geqslant 0$. Finally, we obtain $\|\hat{\mathbf{r}} - \mathbf{A}\mathbf{p}(\tau_n)\|_2^2 \geqslant \|\hat{\mathbf{r}} - \mathbf{A}\mathbf{p}(\tau_{n+1})\|_2^2$.

Appendix C

An alternative interpretation of the residual

The residual correlation $\mathbf{b}$ that appears when the LARS/homotopy algorithm is applied to the problem (4.10), has a clear physical interpretation.

Bearing in mind (4.7), the residual correlation $\mathbf{b}$ when LARS/homotopy is applied to (4.10) takes the form

$$\mathbf{b}(\tau) = \mathbf{A}^T \left(\hat{\mathbf{r}} - \mathbf{A}\mathbf{p}(\tau)\right) = \begin{bmatrix} \tilde{\mathbf{A}}_r^T & \tilde{\mathbf{A}}_i^T \end{bmatrix} \left(\begin{bmatrix} \hat{\mathbf{r}}_r \\ \hat{\mathbf{r}}_i \end{bmatrix} - \begin{bmatrix} \tilde{\mathbf{A}}_r \\ \tilde{\mathbf{A}}_i \end{bmatrix} \mathbf{p}(\tau) \right) \tag{6.8}$$

which can be rewritten in terms of complex matrices $\tilde{\mathbf{A}}$ exposed in (4.6) and the sample covariance $\hat{\mathbf{R}}$.

$$\mathbf{b}(\tau) = \mathrm{Re}\left\{ \tilde{\mathbf{A}}^H \left(\mathrm{vec}\left[\hat{\mathbf{R}}\right] - \tilde{\mathbf{A}}\mathbf{p}(\tau) \right) \right\} \tag{6.9}$$

The term $\tilde{\mathbf{A}}\mathbf{p}(\tau)$ can be expressed as

$$\tilde{\mathbf{A}}\mathbf{p}(\tau) = \begin{bmatrix} \mathbf{s}_1^* \otimes \mathbf{s}_1 & \mathbf{s}_2^* \otimes \mathbf{s}_2 & \cdots & \mathbf{s}_G^* \otimes \mathbf{s}_G \end{bmatrix} \begin{bmatrix} p_1(\tau) \\ p_2(\tau) \\ \vdots \\ p_G(\tau) \end{bmatrix} = \sum_{i=1}^{G} p_i(\tau)\, \mathbf{s}_i^* \otimes \mathbf{s}_i \tag{6.10}$$

Since $\mathbf{s}_i^* \otimes \mathbf{s}_i = \mathrm{vec}(\mathbf{s}_i \mathbf{s}_i^H)$, then $\tilde{\mathbf{A}}\mathbf{p}(\tau) = \mathrm{vec}\left\{ \sum_{i=1}^{G} p_i(\tau)\, \mathbf{s}_i \mathbf{s}_i^H \right\}$

Applying from (6.10) to (6.9) the residual correlation at breakpoint τ yields:

$$\mathbf{b}(\tau) = \mathrm{Re}\left\{\tilde{\mathbf{A}}^H\left(\mathrm{vec}\left[\hat{\mathbf{R}}\right] - \mathrm{vec}\left[\sum_{i=1}^{G} p_i(\tau)\,\mathbf{s}_i\mathbf{s}_i^H\right]\right)\right\} = \mathrm{Re}\left\{\tilde{\mathbf{A}}^H\,\mathrm{vec}\left(\hat{\mathbf{R}} - \sum_{i=1}^{G} p_i(\tau)\,\mathbf{s}_i\mathbf{s}_i^H\right)\right\} \tag{6.11}$$

Bearing in mind the matrix $\tilde{\mathbf{A}}$ presented in (4.6), the last expression can be rewritten as:

$$\begin{aligned}\mathbf{b}(\tau) = \mathrm{Re}\left\{\begin{bmatrix} \mathbf{s}_1^T \otimes \mathbf{s}_1^H \\ \mathbf{s}_2^T \otimes \mathbf{s}_2^H \\ \vdots \\ \mathbf{s}_G^T \otimes \mathbf{s}_G^H \end{bmatrix}\mathrm{vec}\left[\hat{\mathbf{C}}_\tau\right]\right\} &= \mathrm{Re}\left\{\begin{bmatrix} \left(\mathbf{s}_1^T \otimes \mathbf{s}_1^H\right)\mathrm{vec}\left[\hat{\mathbf{C}}_\tau\right] \\ \left(\mathbf{s}_2^T \otimes \mathbf{s}_2^H\right)\mathrm{vec}\left[\hat{\mathbf{C}}_\tau\right] \\ \vdots \\ \left(\mathbf{s}_G^T \otimes \mathbf{s}_G^H\right)\mathrm{vec}\left[\hat{\mathbf{C}}_\tau\right] \end{bmatrix}\right\} \\ &= \mathrm{Re}\left\{\begin{bmatrix} \mathbf{s}_1^H\hat{\mathbf{C}}_\tau\mathbf{s}_1 \\ \mathbf{s}_2^H\hat{\mathbf{C}}_\tau\mathbf{s}_2 \\ \vdots \\ \mathbf{s}_G^H\hat{\mathbf{C}}_\tau\mathbf{s}_G \end{bmatrix}\right\}\end{aligned} \tag{6.12}$$

being $\hat{\mathbf{C}}_\tau = \hat{\mathbf{R}} - \sum_{i=1}^{G} p_i(\tau)\,\mathbf{s}_i\mathbf{s}_i^H$.

The ith component of $\mathbf{b}(\tau)$ is real because it fulfills $\mathbf{s}_i^H\hat{\mathbf{C}}_\tau\mathbf{s}_i = \mathbf{s}_i^H\hat{\mathbf{C}}_\tau^H\mathbf{s}_i$. Therefore, the residual correlation yields:

$$\mathbf{b}(\tau) = \begin{bmatrix} \mathbf{s}_1^H\hat{\mathbf{C}}_\tau\mathbf{s}_1 & \mathbf{s}_2^H\hat{\mathbf{C}}_\tau\mathbf{s}_2 & \cdots & \mathbf{s}_G^H\hat{\mathbf{C}}_\tau\mathbf{s}_G \end{bmatrix}^T \tag{6.13}$$

This result provides an alternative interpretation of the residual correlation. At each breakpoint τ, the corresponding residual $\mathbf{b}(\tau)$ can be seen as the Bartlett estimator applied to the residual covariance matrix $\hat{\mathbf{C}}_\tau = \hat{\mathbf{R}} - \sum_{i=1}^{G} p_i(\tau)\,\mathbf{s}_i\mathbf{s}_i^H$.

Appendix D

The LARS/homotopy for source location

The method operates in an iterative fashion computing the critical regularization parameters $\tau_0 > \tau_1 > \cdots > \tau_{stop} \geqslant 0$ and the associated minimizers $p(\tau_0),\ p(\tau_1), ..., p(\tau_{stop})$ where an inactive component of $\mathbf{p}$ becomes positive or an active element becomes equal to zero. The algorithm is based on the computation of the so-called vector of residual correlations, or just residual correlation, $\mathbf{b}(\tau) = \mathbf{A}^T(\hat{\mathbf{r}} - \mathbf{A}\mathbf{p}(\tau))$ at each iteration. Let $J = \{i \ : p_i \neq 0\}$ denote the support of $\mathbf{p}(\tau)$ or active set and let $I = \{i \ : \ p_i = 0\}$ denote the inactive set. Residual correlations on the support J must all have equal magnitude $\frac{\tau}{2}$, that is $b_j(\tau) = \frac{\tau}{2}$ for $j \in J$, whereas the residual correlations for the inactive elements satisfy $b_i \leqslant \frac{\tau}{2}$ for $i \in I$.

The LARS/homotopy starts with $\mathbf{p} = \mathbf{0}$ which is the solution of (4.10) for all the $\tau \geqslant \tau_0 = 2\max_i \left(\mathbf{A}^T\hat{\mathbf{r}}\right)_i$, being $\left(\mathbf{A}^T\hat{\mathbf{r}}\right)_i$ the i-th component of the vector $\mathbf{A}^T\hat{\mathbf{r}}$, and proceeds in an iterative manner solving reduced-order linear systems. Given the solution at one breakpoint τ_n, denoted by $\mathbf{p}(\tau_n)$, it is possible to construct the solution at the next breakpoint $\mathbf{p}(\tau_{n+1})$ as follows:

$$\mathbf{p}(\tau_{n+1}) = \mathbf{p}(\tau_n) + \gamma\mathbf{u}(\tau_{n+1}) \tag{6.14}$$

being $\mathbf{u}(\tau_{n+1})$ the update direction and $\gamma > 0$ the walking step. It is important to remark that γ depends also on τ_{n+1}. However, herein this dependency is omitted for notational convenience. This step results in a change in the residual correlation of:

$$\mathbf{b}(\tau_{n+1}) = \mathbf{b}(\tau_n) - \gamma\mathbf{A}^T\mathbf{A}\mathbf{u}(\tau_{n+1}) = \mathbf{b}(\tau_n) - \gamma\mathbf{v}(\tau_{n+1}) \tag{6.15}$$

Where the update direction is given by the solution of the following reduced order linear system:

$$\mathbf{A}_J^T \mathbf{A}_J \mathbf{u}_J (\tau_{n+1}) = \mathbf{1_J} \tag{6.16}$$

and $u_i (\tau_{n+1}) = 0$ for the components off of the active set ($u_i (\tau_{n+1}) = 0$ for $i \notin J$ at τ_n). Where $\mathbf{A}_J$ denotes a submatrix of $\mathbf{A}$ consisting of the columns of the elements of the set J and $\mathbf{1}_J$ denotes a column vector of ones with length equal to the cardinality of the set J. The update direction $\mathbf{u}_J (\tau_{n+1}) = \left(\mathbf{A}_J^T \mathbf{A}_J\right)^{-1} \mathbf{1}_J$, also named equiangular direction by Efron et al. in [19], ensures that the maximal components of the residual correlation, those corresponding to the active set, decline equally.

The step size $\gamma > 0$ is calculated as the smallest real number that makes a component of the new residual (6.15) becomes equal in size to the maximal ones or an active component of $\mathbf{p}$ become equal to zero. Formally the step size is determined by (see [17] and [45] for further details):

$$\gamma = \min \{\gamma_1, \gamma_2\} \tag{6.17}$$

γ_1 is defined as $\gamma_1 = \min_{i \in I} \frac{\frac{\tau_n}{2} - \mathbf{b}_i(\tau_n)}{1 - \mathbf{v}_i(\tau_{n+1})}$ and is the minimum step which implies the activation of a zero component of $\mathbf{p}$. The parameter γ_2 is related with the second scenario leading to a breakpoint: when an active component crosses zeros. This occurs when $\gamma_2 = \min_{j \in J} \left\{ -\frac{\mathbf{p}_j(\tau_n)}{\mathbf{u}_j(\tau_{n+1})} \right\}$. It is important to remark that there is only one new candidate to enter or leave the active set at iteration of the algorithm (this condition is the so-called "one at a time condition" by Efron et al. in [19]).

With the new step size the next breakpoint can be obtained as $\tau_{n+1} = \tau_n - 2\gamma$ (since $\gamma > 0$, then $\tau_n > \tau_{n+1}$) and the associated minimizer as $\mathbf{p} (\tau_{n+1}) = \mathbf{p} (\tau_n) + \gamma \mathbf{u} (\tau_{n+1})$. This iterative procedure must be halted when a stopping condition is satisfied.

Bibliography

[1] H. L. V. Trees, *Detection, estimation, and modulation theory, part IV: optimum array processing.* John Wiley & Sons, New York, USA, 2002.

[2] J. Capon, "High-resolution frequency-wavenumber spectrum analysis," *Proc. IEEE*, vol. 57, no. 8, pp. 1408–1418, 1969.

[3] M. A. Lagunas and A. Gasull, "An improved maximum likelihood method for power spectral density estimation," *IEEE Transactions on Acoustics Speech Signal Processing*, vol. ASSP-32, no. 1, pp. 170–173, Feb. 1984.

[4] R. Schmidt, "Multiple emitter location and signal parameter estimation," *IEEE Transactions on Antennas and Propagation*, vol. 34, no. 3, pp. 276–280, 1986.

[5] P. Stoica and A. Nehorai, "Performance study of conditional and unconditional direction-of-arrival estimation," *Acoustics, Speech and Signal Processing, IEEE Transactions on*, vol. 38, no. 10, pp. 1783 –1795, oct 1990.

[6] J. A. Högbom, "Aperture synthesis with a non-regular distribution of interferometer baselines," *Astronomy and Astrohpysics, Suppl. 15*, pp. 417–426, 1974.

[7] P. Stoica and R. Moses, *Spectral analysis of signals.* Prentice Hall, NJ, USA, 2005.

[8] T. E. Tuncer and B. Friedlander, *Classical and modern Direction-of-Arrival estimation.* Elsevier academic press, Burlington, USA, 2009.

[9] P. Charbonnier, L. Blanc-féraud, G. Aubert, and M. Barlaud, "Deterministic edge-preserving regularization in computed imaging," *IEEE Trans. Image Processing*, vol. 6, pp. 298–311, 1997.

[10] H. Zou and T. Hastie, "Regularization and variable selection via the elastic net," *Journal Of The Royal Statistical Society Series B*, vol. 67, no. 2, pp. 301–320, 2005.

[11] D. L. Donoho, "Compressed sensing." *IEEE Transactions on Information Theory*, pp. 1289–1306, 2006.

[12] S. Boyd and L. Vandenberghe, *Convex Optimization*. Cambridge University Press, Mar. 2004.

[13] D. L. Donoho and M. Elad, "Optimally sparse representation in general (nonorthogonal) dictionaries via l1 minimization," *Proceedings of The National Academy of Sciences*, 2003.

[14] D. L. Donoho, "For most large underdetermined systems of equations, the minimal l1-norm near-solution approximates the sparsest near-solution," *Communications on pure and applied mathematics*, vol. 59, no. 7, pp. 907–934, 2006.

[15] R. Tibshirani, "Regression shrinkage and selection via the lasso," *Journal of the Royal Statistical Society, Series B*, vol. 58, pp. 267–288, 1996.

[16] S. S. Chen, D. L. Donoho, Michael, and A. Saunders, "Atomic decomposition by basis pursuit," *SIAM Journal on Scientific Computing*, vol. 20, pp. 33–61, 1998.

[17] D. L. Donoho and Y. Tsaig, "Fast solution of l1-norm minimization problems when the solution may be sparse," *IEEE Transactions on Information Theory*, vol. 54, pp. 4789–4812, 2008.

[18] M. R. Osborne, B. Presnell, and B. A. Turlach, "A new approach to variable selection in least squares problems," *IMA Journal of Numerical Analysis*, vol. 20, no. 3, pp. 389–403, 2000.

[19] B. Efron, T. Hastie, I. Johnstone, and R. Tibshirani, "Least angle regression," *Annals of Statistics*, vol. 32, pp. 407–499, 2004.

[20] I. F. Gorodnitsky and B. D. Rao, "Sparse signal reconstruction from limited data using focuss: A re-weighted minimum norm algorithm," *IEEE Trans. Signal Processing*, pp. 600–616, 1997.

[21] J. Fuchs, "Linear programming in spectral estimation: application to array processing," in *In Proc. ICASSP, vol III*, 1996, pp. 3161–3164.

[22] S. F. Cotter, B. D. Rao, K. E., and K. Kreutz-delgado, "Sparse solutions to linear inverse problems with multiple measurement vectors," *IEEE Trans. Signal Processing*, pp. 2477–2488, 2005.

[23] T. Yardibi, J. Li, P. Stoica, M. Xue, and A. B. Baggeroboer, "Source localization and sensing: A nonparametric iterative adaptive approach based on weighted least squares," *IEEE Trans. on Aerospace and Electronic Systems*, vol. 46, no. 1, pp. 425–443, Jan 2010.

[24] D. M. Malioutov, M. Çetin, and A. S. Willsky, "A sparse signal reconstruction perspective for source localization with sensor arrays," *IEEE Transactions on Signal Processing*, vol. 53, pp. 3010–3022, 2005.

[25] Y. C. Eldar and H. Rauhut, "Saverage case analysis of multichannel sparse recovery using convex relaxation," *IIEEE Trans. Inf. Theory*, vol. 56, no. 1, pp. 505–519, Jan 2010.

[26] T. Yardibi, J. Li, P. Stoica, and L. N. Cattafesta, "Sparsity constrained deconvolution approaches for acoustic source mapping," *Journal of The Acoustical Society of America*, vol. 123, 2008.

[27] J. S. Picard and A. J. Weiss, "Direction finding of multiple emitters by spatial sparsity and linear programming," in *Proceedings of the 9th international conference on Communications and information technologies*, ser. ISCIT'09, 2009, pp. 1258–1262.

[28] P. Stoica, P. Babu, and J. Li, "Spice: A sparse covariance-based estimation method for array processing," *IEEE Transactions on Signal Processing*, vol. 59, no. 2, pp. 629–638, 2011.

[29] Z. Liu, Z. Huang, and Y. Zhou, "Direction-of-arrival estimation of wideband signals via covariance matrix sparse representation," *IEEE Transactions on Signal Processing*, vol. 59, no. 9, pp. 4256–4270, 2011.

[30] P. Stoica, P. Babu, and J. Li, "A sparse covariance-based method for direction of arrival estimation," in *ICASSP*. IEEE, 2011, pp. 2844–2847.

[31] X. Mestre, "Improved Estimation of Eigenvalues and Eigenvectors of Covariance Matrices Using Their Sample Estimates," *IEEE Trans. on Information Theory*, vol. 54, no. 11, pp. 5113–5129, 2008.

[32] H. Akaike, "A new look at the statistical model identification," *IEEE Transactions on automatic control*, vol. 19, pp. 716–723, 1974.

[33] J. Rissanen, "Modeling by shortest data description," *Automatica*, vol. 14, pp. 465–471, 1978.

[34] L. Godara, *Smart Antennas*. CRC Press, 2004.

[35] B. G. Clark, "An efficient implementation of the algorithm 'CLEAN'," *Astronomy and Astrophysics*, vol. 89, no. 3, pp. 377–378, Sept. 1980.

[36] S. S. Young, R. G. Driggers, and E. L. Jacobs, *Signal Processing and Performance Analysis for Imaging Systems*. Artech House, Norwood, MA, 2008.

[37] A. F. R. Bose and B. Steinerg, "Sequence clean: A modified deconvolution technique for microwave images of continuous targets," *IEEE Trans. Aerosp. Electr. Syst.*, vol. 38, pp. 89–96, Jan. 2002.

[38] J. Schmitt, "Restoration of optical coherence images of living tissue using the clean algorithm," *J. Biomed. Opt.*, vol. 3, pp. 66–75, Jan. 1998.

[39] H. Deng, "Effective clean algorithms for performance-enhanced detection of binary coding radar signals," *IEEE Transactions on Signal Processing*, vol. 52, no. 1, pp. 72–78, Jan. 2004.

[40] S. Baisch and G. H. R. Bokelmann, "Spectral analysis with incomplete time series: an example from seismology," *Comput. Geosci.*, vol. 25, pp. 739–750, August 1999.

[41] D. H. Roberts, J. Lehar, and J. W. Dreher, "Time series analysis with clean - part one - derivation of a spectrum," *The Astronomical Journal*, vol. 93, pp. 968–988, 1987.

[42] A. B. Gershman and V. I. Turchin, "Nonwave field processing using sensor array approach," *Signal Process.*, vol. 44, pp. 197–210, June 1995.

[43] U. J. Schwarz, "Mathematical-statistical description of the iterative beam removing technique (method clean)," *Astronomy Astrophysics*, vol. 65, no. 2, pp. 345–356, 1978.

[44] G. Foster, "The Cleanest Fourier spectrum," *Astronomical Journal*, vol. 109, no. 4, pp. 1889–1902, Apr. 1995.

[45] M. Mørup, K. H. Madsen, and L. K. Hansen, "Approximate l0 constrained non-negative matrix and tensor factorization," in *In proc. International Conference on Circuits and Systems, ISCAS 2008*, 2008.

[46] B. W. Rust and D. P. O'Leary, "Residual periodograms for choosing regularization parameters for ill-posed problems," *Inverse Problems*, vol. 24, 2008.

[47] P. Hansen, M. Kilmer, and R. Kjeldsen, "Exploiting residual information in the parameter choice for discrete ill-posed problems," *BIT Numerical Mathematics*, vol. 46, no. 1, pp. 41–59, 2006.

[48] M. Bartlett, *An introduction to Stochastic Processes*. Cambridge University Press, 1966.

[49] J. Durbin, "Tests for serial correlation in regression analysis based on the periodogram of least-squares residuals," *Biometrika*, vol. 56, no. 1, pp. 1–15, 1969.